Diversification of pharmaceutical manufacturing processes: Taking the plunge into the non-PGM catalyst pool

Hui Zhao,[||] Anne K. Ravn,[‡] Michael C. Haibach,*[§] Keary M. Engle,*[‡] Carin C. C. Johansson Seechurn*[†]

AUTHOR ADDRESS [||]Sinocompound Catalysts, Building C, Bonded Area Technology Innovation Zone, Zhangjiagang, Jiangsu 215634, China [‡]Department of Chemistry, The Scripps Research Institute, 10550 North Torrey Pines Road, La Jolla, CA 92037, USA [§]Process Research and Development, AbbVie Inc., 1 North Waukegan Road, North Chicago, Illinois 60064, USA. [†]Sinocompound UK, 14b Warwick Road, Barnet, EN5 5EQ.

KEYWORDS: non-platinum group metals, pharmaceutical industry, earth-abundant metals, catalysis, sustainability

ABSTRACT: Recent global events have led to the cost of platinum group metals (PGMs) reaching unprecedented heights. Many chemical companies are therefore starting to seriously consider and evaluate if, and where, they can substitute PGMs for non-PGMs in their catalytic processes. This review covers recent highly relevant applications of non-PGM catalysts in the modern pharmaceutical industry. By highlighting these selected successful examples of non-PGM-catalyzed processes from the literature, we hope to emphasize the enormous potential of non-PGM catalysis and inspire further development within this field to enable this technology to progress towards manufacturing processes. We also present some historical context and review the perceived advantages and challenges of implementing non-PGM catalysts in the pharmaceutical manufacturing environment.

1. INTRODUCTION

It is well-established that non-precious metal[i] catalysis has been widely utilized since the beginning of the twentieth century for large-scale industrial processes in the petrochemical, food, and fine chemical industries. In addition, essential biochemical transformations in living organisms take advantage of enzymes containing base metal ions, such as iron and magnesium.[1] These examples stand in stark contrast to the state of play in the pharmaceutical industry, wherein platinum group metal (PGM) catalysis is heavily relied upon and adoption of non-PGM alternatives is not yet widespread.

The late twentieth century witnessed a rise in processes catalyzed by platinum group metals (PGMs) in the pharmaceutical industry to construct the frameworks of key intermediates that could not be obtained by traditional synthetic methodology. Subsequently, during the last two decades, PGM catalysis has made substantial contribution to the synthesis of compound libraries in batch as well as flow production, lead optimization, process chemistry and ultimately the large-scale preparation of APIs (active pharmaceutical ingredients) with high efficiency.[2] Indeed, the cherry on the cake for PGM-catalyzed reactions has been recognition with multiple Nobel Prizes in chemistry—for asymmetric hydrogenation and oxidation, olefin metathesis, and cross-coupling reactions. Because catalysts comprised of palladium, rhodium, iridium, platinum, and ruthenium play an important role in the above transformations, it is unsurprising that precious metal catalysts have been selected as more general choices for metal-catalyzed reactions since the 1970s. Today, this trend continues, as indicated by the number of journal publications involving metal catalysis since 1998 (Figure 1), with the most frequently investigated metal being palladium for C-C and C-N bond formation, and ruthenium and rhodium for hydrogenation reactions.

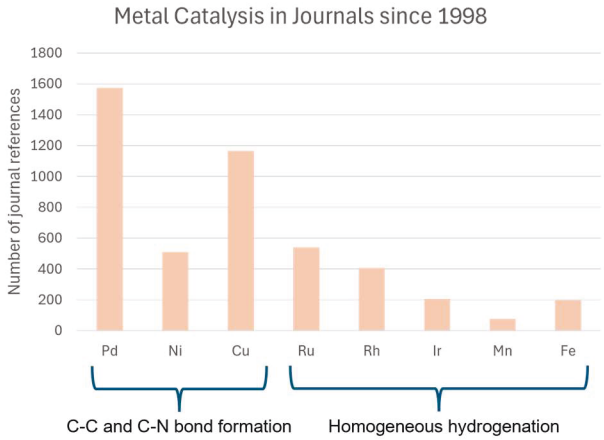

[i] The platinum-group metals (PGMs) (also sometimes referred to as noble metals) are six neighboring transition metals, Ru, Rh, Pd, Os, Ir and Pt. Precious metal is a metal that is relatively rare and hence, has a very high value. Non-PGM metal is any metal other than a platinum-group metal.

Figure 1. Journal publications involving metal catalysis since 1998. Data from SciFinder (search terms: 'metal' AND 'C-C/C-N bond formation' for Pd, Ni, Cu, and 'metal' AND 'homogeneous hydrogenation' for Ru, Rh, Ir, Mn, Fe).

It is interesting to consider that historically, both palladium and nickel catalysts were reported in early examples of C–C cross-coupling reactions. Why did subsequent research for pharma applications of these reactions focus more heavily on palladium? In Negishi's report of the very first Negishi reaction in 1977, both $Ni(PPh_3)_4$ and $PdCl_2(PPh_3)_2$ were successful catalysts for aryl–aryl bond formation. What may have tipped the balance in favor of palladium over nickel could have been a combination of factors, the importance of which slowly emerged over time. First, a key consideration is the need for high functional group tolerance due to the structural complexity of many drugs. The Kumada coupling (1970) is a classic example of a highly efficient Ni-catalyzed reaction with limited functional group tolerance. Second, the ease in which phosphine ligands can be tuned for PGMs, such as palladium, rhodium, and ruthenium, to engender desired reactivity and selectivity profiles proved to be highly enabling; as the importance of ancillary ligands became increasingly understood, the size of the phosphine ligand libraries available for these metals grew very rapidly. Third, an issue that has emerged in relatively recent years stems from the competitive timelines in the pharmaceutical industry combined with the often costly nature of the substrates, particularly in the early drug development phases. R&D and management often face the choice between using a cheaper, but less well-known, process with a non-PGM catalyst, or the use of a more conventional, but more costly, process using a PGM catalyst. Due to the higher potential risk of batch failure when the less conventional (non-PGM) process is used, in many cases the higher cost associated with the PGM-based route can be justified during R&D. Non-PGM catalyzed reactions have less precedence on large scale and are more complex and less understood, which makes quick trouble-shooting more difficult.

Another contributing factor to palladium being heavily favored over nickel for cross-coupling applications in industry has been the availability of readily accessible catalyst precursors. Nickel in particular suffered due to the instability, high cost, and toxicity associated with $Ni(COD)_2$. The relatively slow uptake of nickel-catalyzed processes in industry may have, in turn, influenced academic research efforts to some extent. This effect can arguably also be seen in the massive difference in the range of commercially available phosphine ligands versus that of nitrogen-donor ligands, which in turn presents further challenges to the application of certain nickel and copper-catalyzed processes.

Although the success and synthetic advantages of the use of PGM catalysis is evident, gradually, shortcomings, such as low abundance, high price, and supply insecurity of these precious metals, have become increasingly pertinent considerations, especially with the mounting strain of the global resources and global supply chain. From this point of view, non-precious metal catalysts seem like obvious alternatives due to their advantages over precious counterparts from many practical perspectives (cost, abundance, sustainability, and waste streams[ii]).

As a matter of fact, non-precious metal catalysts have resurfaced in recent years to provide alternatives to precious metals for transformations such as cross-couplings, hydrogenations, oxidations, aminations, alkoxylations, hydrosilylations,[1] and C–H activations.[11] One of the drivers, if not the main driver, behind this surge of papers is the recent spike in metal prices. As shown in Figure 2, recent global events have caused some metal prices to skyrocket, and unfortunately there is no telling whether the price will ever return to the reasonably stable levels prior to 2018. In any case, this has served as a warning signal and spurred researchers on to find potential alternative methods, particularly for transformations that previously relied on PGM-catalysis only and especially for progression into scale-up and manufacturing.

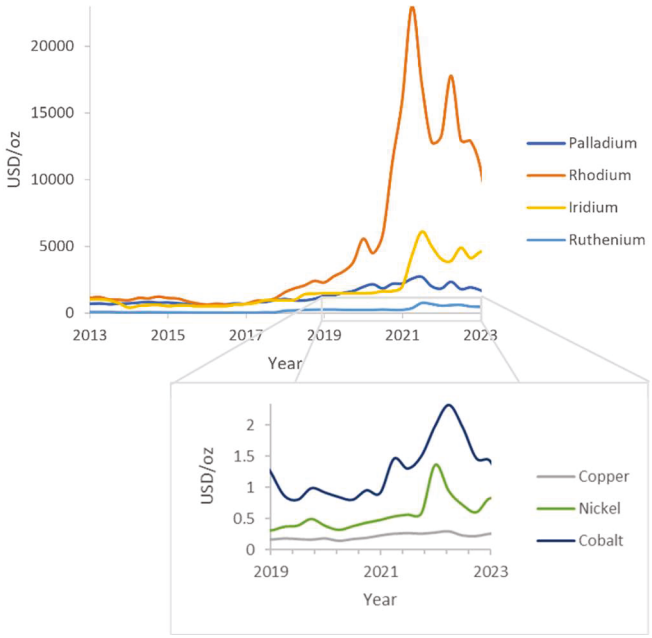

Figure 2. The cost graphs of selected metals over the past 10 years.[12]

The trend of recent interest in non-PGM metal catalysis seems to be common ground for academic and industrial researchers, although, as with most 'new' technologies, surprisingly few have found their way into pharmaceutical scale-up or manufacturing processes. The number of literature reports disclosed by academic groups far outweigh the reports on successful translation of these emerging methodologies to an industry-based user. As shown in Figure 3, the number of literature reports involving non-PGM catalysis increased steadily during the last decade. In 2019, over 16,000 references involving non-PGMs were published. This may be due in part to the availability of research funding. One academic researcher commented a few years back that 'it is increasingly difficult to get funding applications

[ii] See Section 1.1 of this review for additional discussion around waste streams.

approved for proposals that involve PGM catalysis'. The industrial chemist, in his/her turn, faces a number of different challenges, such as robustness, issues with work-up and cost, to proceed via the route less travelled compared to sticking with reliable (but increasingly less sustainable) PGM catalysis.

A thorough review article of non-PGM publication statistics recently appeared as a pre-print, and the interested reader is referred to this publication for more in-depth analysis.[1]

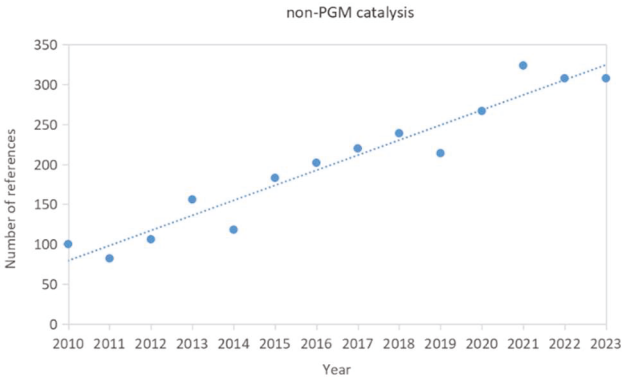

Figure 3. The number of references involving non-PGM metal catalysis increased during the last decades. Data from SciFinder.

Although the study of non-PGM catalysis is flourishing in academia, adoption of these methods in the pharmaceutical industry faces several challenges. These include less well elucidated mechanistic pathways, risk aversion to replace known catalysts with less familiar systems, as well as the difficulty in sourcing some non-PGM catalysts on large scale. Another challenge is that some non-PGM publications require the use of relatively expensive ligands, driving up the overall process cost compared to a potentially competing PGM-catalyzed process. As a hypothetical example, the ligand cost difference would likely outweigh the metal cost difference when comparing BINAP-Ru with DuPhos-Ni for an asymmetric hydrogenation, if the ruthenium loading can be low enough.

There can also be key limits in the substrate scope of non-PGM publications. Sometimes, this methodology may not tolerate electron-rich aryl halides, sterically hindered nucleophiles, or substrates with Lewis-basic functional groups. Non-PGM-catalyzed processes more often require conditions that are difficult to scale up: for example, reactions that require >100 psi hydrogen, anhydrous insoluble bases, insoluble reductants in reductive cross-coupling, multicomponent metallophotoredox protocols or precise water stoichiometry. Finally, since non-PGM-catalyzed reactions are more recent and emerging technologies, they are also more likely to be covered by IP (both composition of matter and use patents) than more established PGM-catalyzed reactions.

Historically, hesitance to adopt emerging non-PGM catalysis in industry may have stemmed from another interesting reason. Several high-profile cases of reactions that were initially claimed as "non-metal-" or "non-PGM-catalyzed" processes were later proven to be catalyzed by ppm levels of precious metal contaminants in the catalyst, ligand, or other components of the reaction mixture.[1] These examples may have led to unfair levels of skepticism regarding non-PGM catalysis in pharma, though anecdotal evidence suggests that this viewpoint has subsided.

With these challenges in mind, we see increasing evidence that pharmaceutical chemists are pursuing non-PGM catalysis—likely because of large potential economic advantages of non-PGM metal catalysts in comparison to their precious metal analogues. Scientists at Abbvie, Pfizer, and Boehringer Ingelheim have initiated a series of reviews highlighting the progress of non-precious-metal-catalyzed transformations, with the first article published in 2019.[1] These companies also participate in a precompetitive research alliance on non-PGM catalysis, which has resulted in the development of new methods. Iron complexes have been successfully field-tested as highly effective catalysts in practical, kilogram-scale industrial synthesis of pharmaceuticals.[1]

Meanwhile, some truly novel reactions specific to non-PGMs have been developed in the last decade. One key example is the efficient nickel-catalyzed cross-coupling of C–O and C–N bonds of phenol, amide, and ester electrophiles developed by Garg and co-workers.[1] Despite the use of relatively cheap phenol derivatives as starting materials, these Ni-catalyzed cross-couplings have not yet found widespread large-scale use in industry. One possible reason for this is that there are patents covering this type of reaction, which can be a deterrent when developing a potential manufacturing process.[1] Nonetheless, it is worth emphasizing that non-PGM catalysis has the potential to enable entirely novel disconnections, that cannot be realized using PGM catalysis, and provide access to significantly shorter synthesis routes.

Before discussing specific applications of non-PGM catalysis, however, we first want to discuss some common perceived advantages and disadvantages from an industrial perspective. A couple of noteworthy perspectives on the topic of base metal or non-PGM catalysis have been published recently.[1]

1.1. Are non-PGMs more sustainable than PGMs?

There is an increasing focus on sustainable manufacturing within the pharmaceutical industry. [2] A result is the greater attention to the origin and life cycle of all raw materials, including metal catalysts. Often, the word 'sustainable' is used as shorthand for 'environmentally friendly'.[21] However, for a process to qualify as sustainable, other criteria need to be fulfilled as well. As shown in Figure 4, the 'three circles' model of sustainability nicely illustrates this.

Entry	Element	CO_2 emission (kg CO_2 eq per kg metal)[22]	Crustal abundance (ppm)[2]	Annual production (tonnes)	Top 3 producers[2]
1	Pd	3,880	0.015	210[2]	1.South Africa 2.Russia 3.Zimbabwe
2	Ir	8,860	0.001	7[2]	1.South Africa 2.Russia 3.Zimbabwe
3	Rh	35,800	0.001	30[2]	1.South Africa 2.Russia 3.Zimbabwe
4	Ru	2,110	0.001	30[2]	1.South Africa 2.Russia 3.Zimbabwe
5	Ni	6.5	84	2,700,000[2]	1.Russia 2.Indonesia 3.Philippines
6	Cu	2.8	60	21,000,000[29]	1.Chile 2.Peru 3.China
7	Co	8.3	25	170,000[29]	1.DRC 2.China 3.Zambia

Table 1. Sustainability data for selected PGMs and non-PGMs.

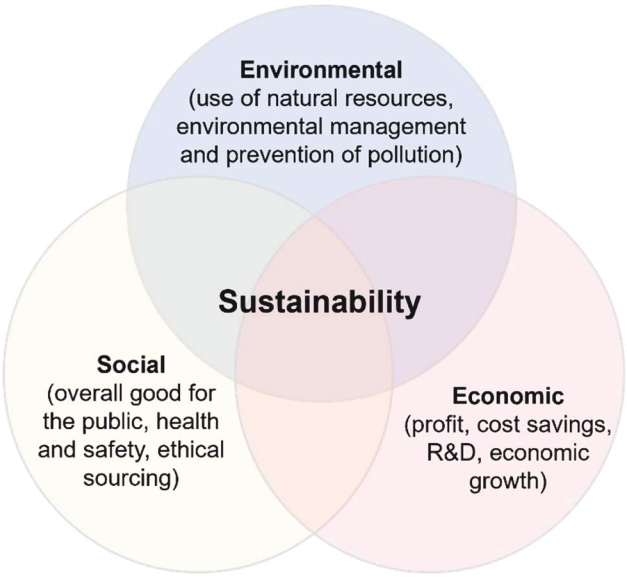

Figure 4. The 'three circles' model of sustainability.

It is noteworthy that catalysis in general is accepted as one of the '12 principles of Green Chemistry', as originally proposed by Paul Anastas and John Warner.

Going into more detail, the fairest way to compare the sustainability of PGMs versus non-PGMs would be to assume that a particular process is using identical conditions, and that the only difference is the use of, for example, palladium in one process and nickel in the other. This is unlikely, however, to be the case in the real world, since the optimal reaction conditions (solvent, base, temperature, etc.) may not be the same for both metals.

A recent perspective by Drover and coworkers discusses the topic of sustainability of precious metals versus base metals. [1] The authors proposed that the definition of a base metal also includes the origin and the ethical mining of the metal, in addition to its natural abundance.

While a full analysis of the supply chain and lifecycle for each of the metals is outside the scope of the present review, we highlight a few key sustainability metrics in Table 1. In terms of global warming potential, the differences can be stark: production of PGMs requires 1,000–10,000 more CO_2 equivalents than non-PGMs.[22]

The disposal of metal-contaminated waste from a pharmaceutical process is part of the metal's life cycle and thus a component of the sustainability question. Waste streams containing PGMs are typically combined for recovery by a specialized company, while non-PGMs are not. [2] Recovery rates for heterogeneous catalysts are ~90%, while those from solution are lower. Both PGMs and non-PGMs may need to be purged from aqueous waste streams due to their aquatic toxicity. When compared in isolation, PGMs may appear advantageous at this stage due to the common use of a recovery step, which is motivated by the cost of the metal but also provides waste remediation. Waste remediation for a non-PGM would thus be an added expense, though the

overall process may still represent a considerable sustainability advantage.

1.2. The toxicity of PGMs vs non-PGMs

It is worth briefly discussing the topic of "toxicity" relating to non-PGM catalysts, since this has historically been an argument used in favor of certain elements (primarily iron and copper). We first refer the reader to a series of perspectives by Egorova and Ananikov; upon reviewing extensive toxicology data, the authors conclude that "*there are no catalytically demanded metals for which comprehensive toxic "portraits" could be built*". The authors therefore argue against using toxicity as selling point for new catalysts.

From the perspective of pharmaceutical manufacturing, there are two main areas of consideration when assessing metal catalyst toxicity: occupational safety and residual metal level in the final product.

The permitted level of residual metal impurities depends on the way the drug is administered; orally, by injection (parenteral) or by inhalation. Generally, the permitted levels of catalytically relevant non-PGMs are higher than those of PGMs (except for cobalt). Palladium, iridium, rhodium, and ruthenium all have the same permitted levels for oral drugs (100 μg/day), parenteral drugs (10 μg/day) and drugs administered by inhalation (1 μg/day) (Table 2, Entries 1–4). Nickel and copper are both permitted to a somewhat higher level; 200 and 2000 μg/day, respectively, for oral drugs, 20 and 300 μg/day, respectively, for drugs that are injected and 5 and 30 μg/day, respectively, for drugs that are administered by inhalation (Entries 5 and 6). Cobalt is more controlled, with permitted levels of 50 μg/day for oral drugs, 5 μg/day for parenteral drugs and 3 μg/day for drugs that are inhaled (Entry 7). Iron does not have a specified PDE (permitted daily exposure) and is treated as an "ordinary" impurity in most scenarios.

Entry	Element	Oral PDE (μg/day)	Parenteral PDE (μg/day)	Inhalation PDE (μg/day)
1	Pd	100	10	1
2	Ir	100	10	1
3	Rh	100	10	1
4	Ru	100	10	1
5	Ni	200	20	5
6	Cu	3000	300	30
7	Co	50	5	3

Table 2. PDE for elemental impurities from ICH Q3D.

Metals with lower PDEs can require more intensive processes for their removal. The ease and cost for removing PGMs or non-PGMs from reaction streams for APIs must be considered as part of the overall cost and sustainability for their application. While various methods for PGM removal have been developed, the removal processes of non-PGMs are less refined, although promising studies have been reported.

The aspect of occupational safety of non-PGMs is less uniformly regulated. In the EU, there are increased regulations on the use of nickel catalysis from this perspective since all nickel compounds are restricted under REACH. Discussions are also on-going regarding REACH regulations for cobalt and some of its inorganic compounds. This can result in a specific process being viable to run in a manufacturing plant in Asia or North America, but not in Europe.

1.3 History of non-PGM in Industrial Processes

Non-PGM catalysis has played an integral part in the synthesis of fine chemicals for many years. Both homogeneous and heterogeneous catalysts derived from non-PGMs have been employed in several extremely important processes in the chemical industry, as exemplified by the Haber–Bosch process (heterogeneous iron), the production of syngas (heterogeneous nickel), the Dupont adiponitrile process (homogenous nickel), and the Shell Higher Olefin Process (homogenous nickel). This list is not exhaustive but nevertheless demonstrates the impact of non-PGMs to produce feedstock and fine chemicals on very large scale.

Haber Process

The famous Haber process (also known as Haber–Bosch process) is the reaction of nitrogen and hydrogen under high temperature and pressure, over a heterogenous iron catalyst, to produce ammonia (Figure 5). It was not until the start of the twentieth century that this method was developed to harness the atmospheric abundance of nitrogen to produce ammonia, which can then be oxidized to make the nitrates and nitrites essential to produce nitrate fertilizer and munitions. Today, over 450 million tons of nitrate fertilizer are produced annually, and it is estimated that 50% of all food grown on the planet is aided by this fertilizer.

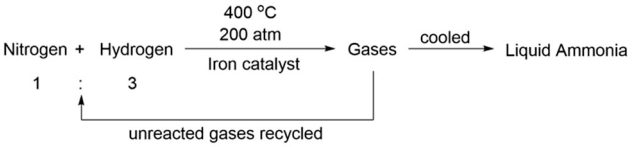

Figure 5. Haber–Bosch process.

Syngas Synthesis

Syngas is a fuel source that mainly consists of hydrogen and carbon monoxide. One of the most important applications of syngas is the usage of it as a feedstock to produce an impressive number of modern industrial chemicals. Notably the synthesis and downstream application of syngas are highly dependent on non-PGM catalysis (Figure 6). One typical process in syngas synthesis is termed steam reforming, which generates hydrogen-rich synthesis gas from light carbohydrates by means of nickel catalysis. Furthermore, the Fischer–Tropsch process that produces synthetic fuels relies on cobalt or iron catalysis. Meanwhile, as the main industrial process for production of hydrogen, the water gas shift reaction (WGSR) relies heavily upon iron- and copper-based catalysts. [1]

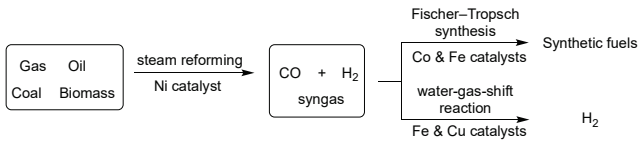

Figure 6. Both synthesis and the downstream application of syngas rely on non-PGM catalysis.

The DuPont adiponitrile process

A historically prominent nickel-catalyzed reaction is the olefin hydrocyanation reaction developed by DuPont to produce adiponitrile (Figure 7). This is an important precursor in the manufacture of nylon. [2]

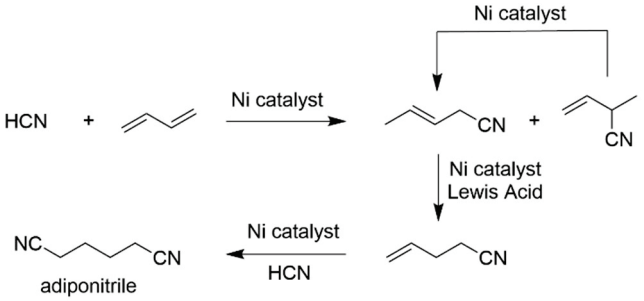

Figure 7. Dupont's Ni-catalyzed hydrocyanation reaction.

The process utilizes nickel(0)–phosphite complexes, such as $Ni[P(O\text{-}o\text{-}tol)_3]_4$, as catalysts for direct addition of HCN to butadiene, followed by a second anti-Markovnikov addition of HCN to produce adiponitrile. This is the main route by which DuPont manufactures adiponitrile in the US. Since 1977, this process is also run in France together by DuPont and Rhone-Poulenc, with an annual capacity of 100,000 tonnes.

On an interesting side note, one of the first applications of the bidentate phosphine ligands XantPhos and DPEPhos, which are now commonly used ligands in Pd-catalyzed cross-coupling reactions, was in the Ni-catalyzed hydrocyanation of alkenes. ,

Shell Higher Olefin Process (SHOP)

Non-PGM catalysis has been widely applied in the petrochemical industry for several decades. Ziegler–Natta catalysts, a broad family that includes titanium complexes, have been employed to catalyze polymerization of ethylene to produce polyethylene (PE). 90% of the high-density polyethylene (HDPE) in the world is produced using Ziegler–Natta catalysts. The synthesis of advanced polymers, e.g. Linear low-density polyethylene (LLDPE), requires extensive use of homogeneous base metal catalysts. SHOP, that was discovered as early as 1968, was achieved by means of nickel-catalyzed oligomerization and metathesis of ethylene. As shown in Figure 8, the nickel–phosphine catalyst **A** is generated in-situ from a nickel salt, $NaBH_4$, a P,O-ligand, and ethylene. Currently, over one million tonnes of C12–C18 α-olefins are manufactured every year using SHOP.[46] As demand for specialty polymers increases, metallocene catalysts are growing in significance. In 2009, a zirconium catalyst was put into operation in the 150,000 metric ton α-Sablin process in Saudi Arabia. Mitsui Petrochemical also developed a homogenous catalytic process with titanium-based catalysts.

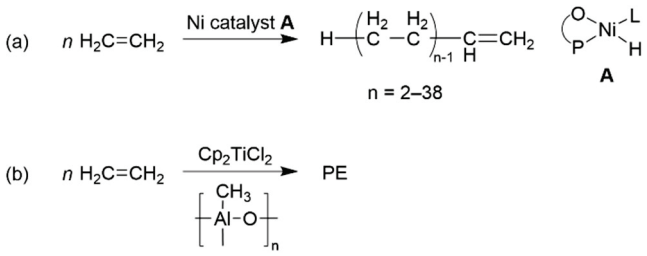

Figure 8. (a) Ni-catalyzed ethylene oligomerization to α-olefins; (b) metallocene-catalyzed polymerization.

Other noteworthy applications

In addition to the non-PGM catalysts mentioned above that have been used for a long time, vanadium has also been used as a chemical catalyst for sulfuric acid production for over 100 years. Aluminosilicates are a critical component of modern petrochemical manufacturing. [1] Sometimes, in the case of heterogeneous catalysis, the nature of the support can have a significant impact on catalytic properties and aluminum can be used for this purpose in the shape of alumina (Al_2O_3). Platinum supported on alumina are highly effective heterogeneous catalysts allowing for the dehydrogenation of alkanes. [2] Olefin hydroformylation represents a large-volume application of catalysis. Originally, this process was achieved using cobalt catalysis, however, high pressure was required to drive these reactions forward. Now, rhodium-based catalysts are more commonly used since lower pressure can then be applied.

In the fuel cell industry, there has been significant research in the replacement of the commonly used platinum-based electrocatalysts with non-PGM-based ones (iron, cobalt, etc.). This would be a major step forward to produce hydrogen from water and renewable energy.

2. NON-PGM CATALYSIS RELEVANT TO THE PHARMACEUTICAL INDUSTRY

As exemplified throughout the following sections of this article, the introduction of non-PGM catalysis in other chemical sectors, including the pharmaceutical industry, is now becoming increasingly apparent. In this section selected examples from the literature are discussed that illustrate emerging trends for the metals highlighted below. The selection of examples focuses on large-scale [iii] or especially pharmaceutically relevant applications of non-PGM-catalyzed reactions.

2.1. Nickel

The smaller size and decreased electronegativity of nickel relative to palladium enables much more facile oxidative addition to weak electrophiles. Beginning in the 1990s, reports emerged demonstrating that nickel catalysts were effective for cross-couplings of aryl methanesulfonate esters. More recently, several groups have developed the nickel-catalyzed cross-coupling of aryl alkyl ethers, benzylic ethers, and certain amides. This advantage among others of nickel catalysis for cross-couplings have prompted researchers to consider its use for large-scale applications.

[iii] Large-scale is defined as ~100 g or greater, except for examples that show the synthesis of radiolabeled compounds (which are usually done at 1-100 g scale in pharma).

In 2015, Jarvo et al. reported a nickel-catalyzed gram-scale Kumada cross-coupling reaction of benzylic ether substrates (Figure 9, equation 1). Using a bidentate nickel catalyst (*rac*-BINAP)$NiCl_2$, the reactions proceed with inversion at the benzylic position, providing the corresponding ring-opened product **2** with high stereospecificity. As shown in Figure 9, equation 2, changing the nickel catalyst to $Ni(COD)_2$ (or $Ni(dppe)Cl_2$), the methodology can be used to synthesize ring-opened products with isotopically labeled substituents, such as **4**. The reaction was demonstrated on multigram scale, with high yield and stereospecificity maintained. This reaction is expected to find use for the preparation of isotopologues of API intermediates, provided that their functional groups tolerate the presence of a Grignard reagent.

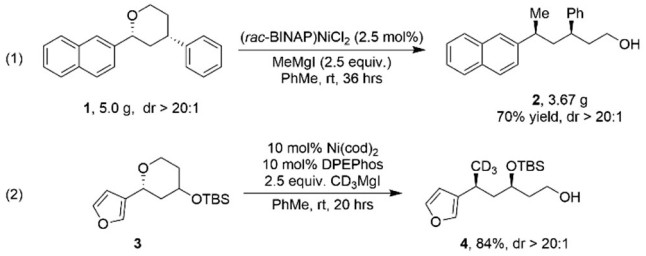

Figure 9. Nickel-catalyzed gram-scale Kumada cross-coupling reactions of benzylic ethers.

As with many other reports from academic settings, it is often only a matter of time before an industrial chemist identifies one of these methodologies as potentially useful for a target structure and sets to work to implement it. The other important function of publications like this is to provide a foundation for, or inspire, further developments within the field to identify other useful transformations. The above example highlights a selected example from the advances in the field within the academic setting. There are numerous other reports that have been crucial to the overall advancement and understanding of the non-PGM catalysis area. Nevertheless, the focus of this review will lie on the development and implementation of this technology for larger scale purposes in industry.

In 2010, scientists at BMS developed a process taking advantage of the catalyst $Ni(acac)_2$ to produce multikilogram quantities of alkenyl bromide **6** (Scheme 1), a key intermediate for the synthesis of alkene derivative **7** that has attractive properties as estrogen agonist/antagonist which are desirable for the treatment of breast cancer. With a relatively high loading of the inexpensive $Ni(acac)_2$ (25 mol%), carbometallation of but-1-ynylbenzene **5** with diphenylzinc/diethylzinc can proceed under moderate temperature, followed by bromination with *N*,*N*'-dibromo-5,5-dimethylhydantoin under well-defined conditions, yielding **6** in 65% isolated yield with high stereoselectivity (Scheme 1). After subsequent recrystallization, **6** can be obtained at 99.3% purity with only <0.1% diethyl analogue and none of the (*E*)-isomer detected. The ease by which the synthesis of **6** can be scaled-up, combined with the commercial availability of the other two synthons enlisted subsequently, (4-formylphenyl)boronic acid and methyl 2-(dimethoxyphosphoryl) acetate, ensured the production of enough **7** for pharmaceutical development activities and clinical trials.

Scheme 1. Kg scale stereoselective synthesis of **6**.

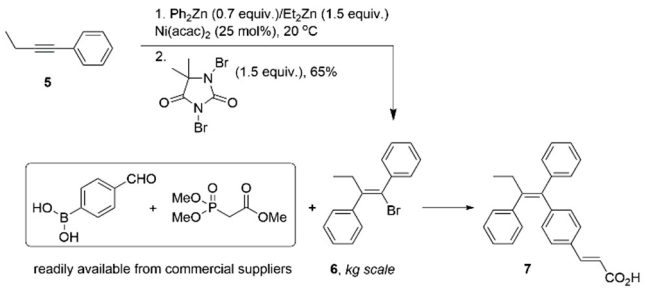

Another example reflecting the economic benefits of nickel is the nickel-catalyzed Suzuki–Miyaura cross-coupling reaction to form **10**, a key intermediate to produce pictilisib, which was achieved on multikilogram-scale. As shown in Scheme 2, Pictilisib, also known as GDC-0941, is a novel small molecule PI3K inhibitor discovered by Genentech, and was evaluated as an anticancer agent. The Suzuki-Miyaura reaction between substrates **8** and **9** was developed initially to produce substantial amounts of GDC-0941 used for supporting further pharmaceutical development activities. The team developed both $PdCl_2(PPh_3)_2$ and $Ni(NO_3)_2{\cdot}6H_2O/PPh_3$ as efficient catalysts for this late-stage cross coupling.

The decision about what catalyst to use ultimately depends on the following factors: substrate performance and the cost of removing impurities. On both points, the route with the nickel precatalyst, which afforded the THP protected **10** in 79% yield, won out over the palladium catalyzed route (Scheme 2). The removal of the residual palladium contaminant required the use of relatively expensive scavengers (Florisil and Thio-Silica) and large volume of solvents; in contrast, the residual nickel catalyst could be easily removed from the crude reaction mixture through an aqueous ammonia wash and crystallization. Moreover, the precatalyst $Ni(NO_3)_2{\cdot}6H_2O$ is relatively cheap (ca. $15/mol) and readily available. Furthermore, the cross-coupling could be operated at an impressive 0.03 mol% catalyst loading.

Scheme 2. Two methods used for the kg scale synthesis of key intermediate **10** and the synthesis of pictilisib.

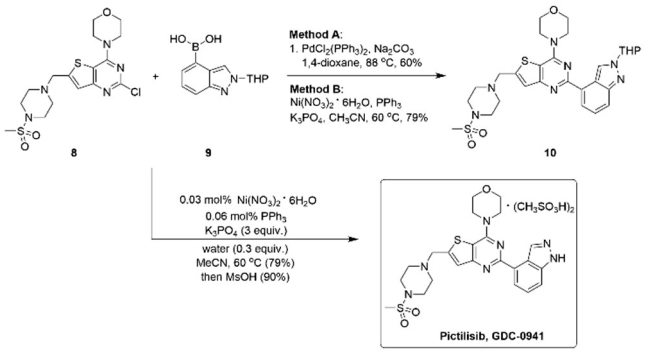

In precious-metal-catalyzed reactions, it is common that the identity of the ancillary ligands can influence product selectivity, and the same is true for non-PGM-catalyzed reactions. Taking the nickel(0)-catalyzed reaction of isocyanates **11** and isatoic anhydrides **12** as an example, screening reaction showed changes in the substitution pattern of the isocyanate led to different products. XantPhos was unique to forming the benzoxazinone imine **13**, while PHOX ligand

allowed for synthesis of the constitutionally isomeric quinazolinediones **14** in excellent yields and selectivities (Figure 10). [1] Both reactions can be performed at gram scale. This example nicely illustrates that the development of general processes for base-metal catalysis also requires highly efficient catalyst and reaction screening systems, similar to those commonly used in PGM-catalyzed reaction development. The difference may be that there is currently less knowledge around which ligands may be effective in combination with non-PGM catalysts in a specific transformation. This can turn a non-PGM catalysis screening project into more of a 'guess-work' and less of a knowledge-based project.

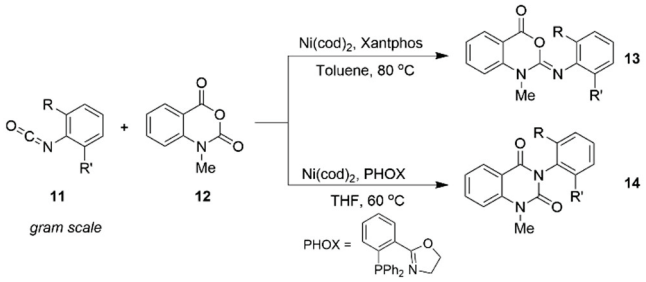

Figure 10. Switching ligands allowed for access to either of the constitutionally isomeric products shown.

Recognizing the value of testing a diverse collection of ligands during the initial evaluation of nickel catalysis in a potential transformation of interest, chemists at BMS reported the development of a 24-reaction screening platform for identifying nickel-catalyzed Suzuki-Miyaura reaction conditions. [2] The screening platform includes $NiCl_2 \cdot 6H_2O$ as catalyst and 12 monophosphine and bisphosphine ligands. The crucial part of this platform is the methanol additive that significantly improves the reaction performance and enables the use of organic-soluble amine bases. (Scheme 3). The ligand screening platform enabled rapid ligand screening for API synthesis with nickel catalysis, as demonstrated by a gram-scale coupling reaction of the antipsychotic perphenazine **15** with boronic acid **16** to form **17** in 83% yield. This methodology was designed to be directly applicable to process scale-up by achieving homogeneous reaction conditions employing stable and inexpensive nickel(II) precatalysts.

Scheme 3. Screening of the boronic acids and aryl halides in Suzuki-Miyaura coupling reactions and gram-scale synthesis of **17**.

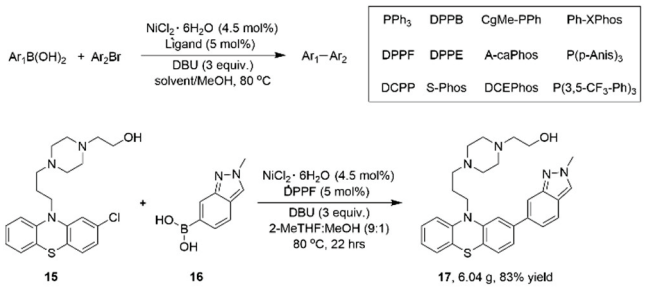

Following their demonstration of homogeneous conditions (MeOH and DBU) for nickel Suzuki-Miyaura reaction, BMS researchers sought to develop aqueous conditions that more closely mimicked those used in the palladium version. Previously, this was challenging for nickel due to the formation of inactive Ni-hydroxide species. As shown in Scheme 4, the authors found that amine bases allowed the nickel-hydroxide formation to be more reversible than with traditional inorganic bases, and conditions were developed with *i*-Pr_2NEt in 2-MeTHF/water. The reaction was catalyzed by a combination of phosphine ligand and the versatile, air-stable nickel precursor, $(PPh_3)_2Ni(o\text{-tolyl})Cl$. DPPB (1,4-bis(diphenylphosphino)butane) had the most generality as the ancillary ligand, though in some cases other common phosphines were optimal. The authors demonstrated an impressive substrate scope containing pharmaceutically derived or relevant heteroaryl-boronic acids and aryl chlorides. An example was demonstrated by a Suzuki-Miyaura cross-coupling reaction on 50 g of pherphenezine **21** using only 0.5 mol% Ni, and the product **23** was isolated by salt formation with only 10 ppm residual nickel (Scheme 5).

Scheme 4. Ni-catalyzed Suzuki-Miyaura reaction of heteroarylboroic acids under aqueous conditions.

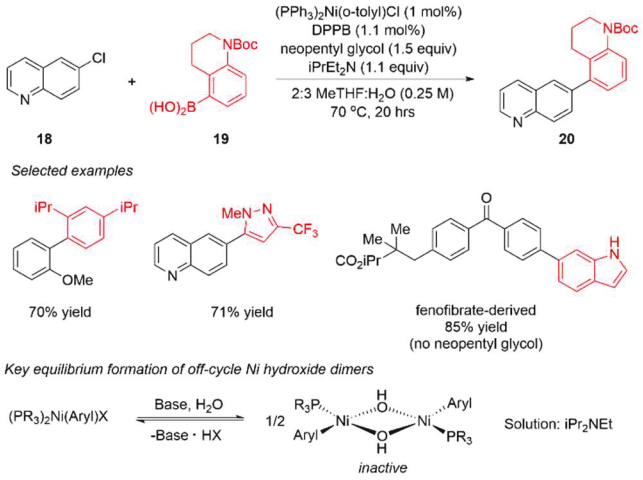

Scheme 5. Perphenazine cross-coupling on a 50 g scale.

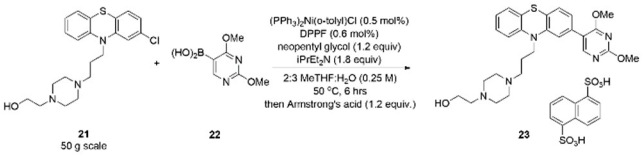

These two examples from the groups at BMS illustrate how demands posed by industrial applications led to advancement of synthetic methodology—in both cases, addressing the need for easily scalable reaction conditions and applicability to decorated heterocyclic substrates. In a similar vein, a collaboration between scientists at AbbVie and Pfizer sought to address another major limitation of the Ni-catalyzed Suzuki-Miyaura reaction: poor reactivity with Lewis-basic arylboron nucleophiles. The authors found that the majority of widely studied phosphine/Ni catalysts were unable to promote the coupling of a (pyridyl)Bpin **24**, while the simple ligand PPh_2Me was highly effective. The reactions, which were performed from mg to g scale, proceed under "standard" palladium-catalyzed Suzuki-Miyaura reaction conditions with K_3PO_4 as base in 2-MeTHF/water as the solvent (Scheme 6). Under these conditions, many Lewis basic (aryl)Bpin substrates could be coupled with functionalized heteroaryl halides in moderate to high yield. The

active catalyst $(PPh_2Me)_4Ni$ was generated by mixing $(PPh_2Me)_2NiCl_2$, PPh_2Me and *n*-BuMgCl, though $(PPh_2Me)_2Ni$(o-tolyl)Cl, PPh_2Me and (TMEDA)Ni(*o*-tolyl)Cl were also effective catalysts. The surprising activity of PPh_2Me was shown to result part from the ability of this ligand to resist substitution by Lewis basic substrates at Ni(aryl)X intermediates.

Scheme 6. Ni-catalyzed small scale Suzuki-Miyaura reaction of Lewis basic aryl-Bpin substrates **24** under aqueous conditions.

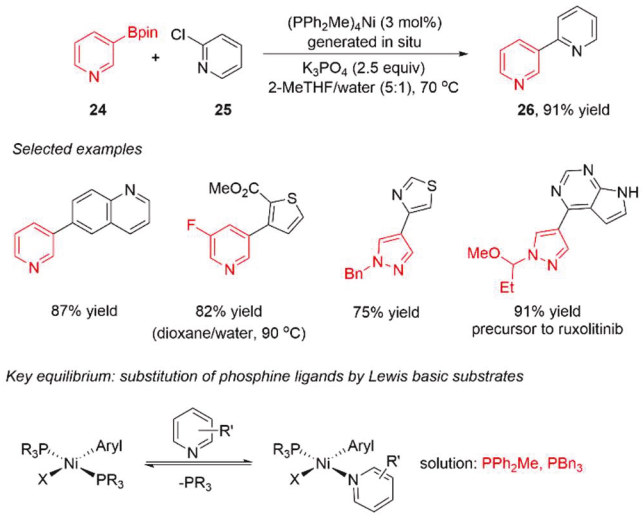

Nickel catalysis has also found industrial relevance in other cases involving challenging nucleophiles. In 2016, scientists at Bayer reported a mg scale nickel-catalyzed cyanation of aryl halides **27**. As shown in Scheme 7, the reaction uses the recently developed (TMEDA)NiCl(*o*-tolyl) as the precatalyst and bidentate phosphine dppf as the ligand. These reactions were run in 2-propanol as the solvent using DIPEA as a base at 80 °C, leading to reaction completion typically within two hours, providing simple benzonitriles **28** in moderate to excellent yield. Interestingly, the reaction conditions are analogous to those of palladium-catalyzed reaction systems. Most simple electron-deficient aryl bromides are well-tolerated, while aryl chlorides and electron-rich aryl bromides gave low to no conversion. The authors pointed out that although the scope of nickel-catalyzed cyanation demonstrated to date is not as extensive compared to that of palladium-based methods, the operational simplicity coupled with the low cost of nickel will facilitate the development of this method to produce simple aryl nitriles on an industrial scale. An additional advantage is the use of acetone cyanohydrin (ACH) as the cyanide source, which is safer to handle than for example HCN

Scheme 7. Mg scale synthesis of simple benzonitriles **28** by nickel-catalyzed cyanation of aryl halides.

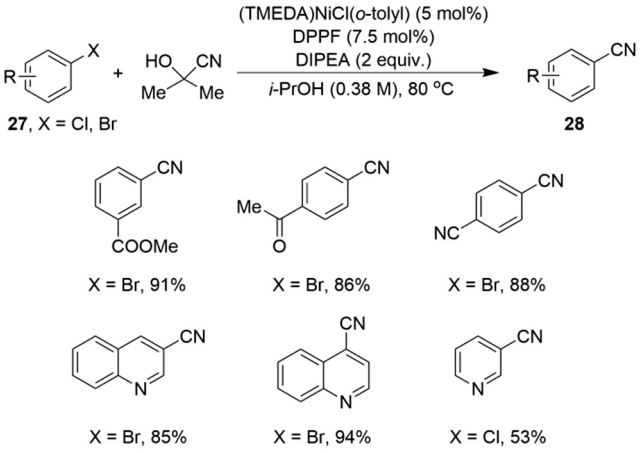

In 2024, researchers at Merck described their efforts in developing a robust, and scalable nickel-catalyzed sulfonylation of **29** to access intermediate **30** as a means to identify a more sustainable and cost-effective manufacturing process of the API Belzutifan (Scheme 8). The previous process had utilized copper-catalysis and sodium methanesulfinate for the sulfonylation, but this reagent was costly for the overall synthesis. The inorganic sulfur salt, potassium metabisulfite, was chosen as an inexpensive source of SO_2, however, the reagent introduced stirring challenges due to heterogeneity of the reaction. Slow addition of the reductant, potassium formate, in ethylene glycol mitigated these mixing challenges which ultimately allowed for the lowering of the amount of metabisulfite. This prevented catalyst poisoning with SO_2, thus lowering the catalyst loading to 5 mol% $NiCl_2$(dppe). Furthermore, the versatile nickel catalyst system was amenable to in situ methylation conditions of the aryl sulfinate using the nontoxic reagent trimethylphosphate thereby circumventing the need for subsequent methylation. The process was demonstrated on 3 kg scale, providing 76% yield of the desired product **30**.

Scheme 8. Ni-catalyzed sulfonylation reaction of aryl bromide **26** to intermediate **27** in the manufacturing process of API Belzufan.

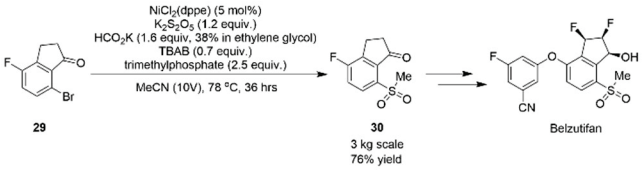

The combination of air-stable nickel catalyst precursors and phenanthroline ligands also enables the direct arylation of pyridine substrates using non-PGM catalysts. Chemists at Boehringer Ingelheim reported the first mg scale nickel-catalyzed C-3 direct arylation of pyridinium ion substrates (**31**), which was found to enable access to azafluorene pharmacophores (Scheme 9). This methodology, combining commercially available $NiCl_2$(DME) as catalyst and inexpensive 1,10-phenanthroline as ligand, is compatible with a variety of substituents either on the aryl halide or pyridine core. As shown in Scheme 7, substrates with either electron-withdrawing substituents at C-6, such as esters **32a**, amides **32b**, nitriles **32c** and sulfonamides **32d,** or substituents at

C-4 of the pyridine ring **32e** were well tolerated (77–95%). After debenzylation and reduction, the *N*-benzyl protected 1-azafluorenes can afford valuable pharmacophores, such as **33** and **34** (Scheme 10). Notably, the debenzylation step still requires the use of a palladium catalyst, highlighting the remaining PGM-dependency of this synthesis route.

Scheme 9. Nickel-catalyzed C-3 direct arylation of pyridine derivatives **31** at mg scale**.**

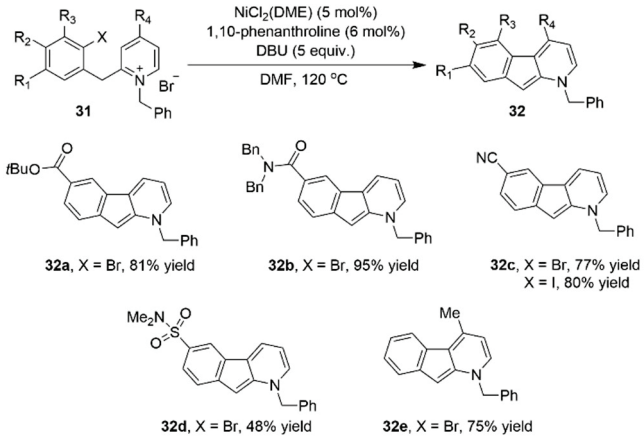

Scheme 10. Debenzylation and reduction of 1-azafluorenes 32a to valuable pharmacophores **33** and **34**.

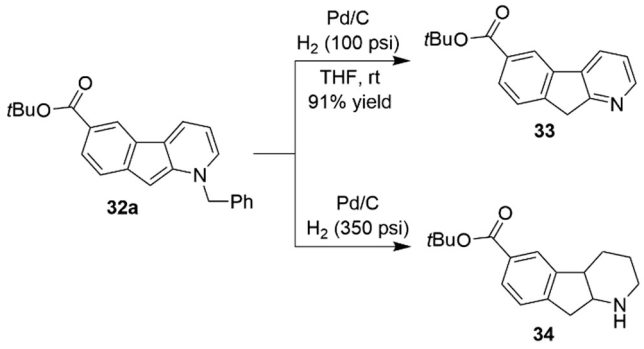

Another reported example of nickel-catalysis utilized to selectively construct cyclized structures is in the formation of the nitrogen-rich heterocycle core of the JAK2 inhibitor BMS-911543. The scientists at BMS found that under low pressure hydrogen using $Ni(acac)_2(H_2O)_2$ with nickel oxide supported on silica (PRICAT), the C–N cyclization of pyrrole and activated hydroxylamine in compound **35** was observed in 77% yield and 16:1 selectivity for the desired cyclized product **36** (Scheme 11). This method provided a fruitful route for the heterocyclic core, which had been unsuccessful to construct via 6π-electrocyclization pathways. Notably, no product was obtained if using unsupported $Ni(acac)_2(H_2O)_2$.

Scheme 11. Nickel-catalyzed C–H functionalization in the synthesis of BMS-911543 at gram scale.

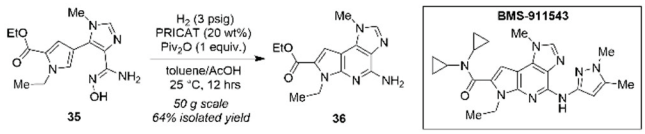

In 2020, researchers at BMS described a practical method taking advantage of a nickel-catalyzed reductive cross-coupling strategy for the kg scale synthesis of **39**, a key intermediate towards dihydroquinolinone core structures (Scheme 12). Initial experiments showed that the Pd-catalyzed Negishi cross-coupling afforded the desired product in 65% conversion; however, the limited availability of the organozinc species on large scale proved to be a constraint. Suzuki- and Heck-based strategies also failed. Fortunately, catalyst and ligand screening revealed that the combination of $NiCl_2$(DME) and 1,10-phenanthroline was the best catalytic system for the reductive coupling of 2-chloropyridine **37** and ethyl 3-chloropropanoate **38**. In addition, stoichiometric manganese as the terminal reductant and chlorotriethylsilane (TESCl) as the activator provided an optimal conversion. The process was demonstrated on a 7 kg scale and afforded **39** in 64% yield. Obviously, a comprehensive understanding of mixing requirements, including maintaining an optimal suspension of the manganese to promote catalytic turnover and identifying the appropriate agitation parameters through modeling, was important for the successful scale-up of this reaction.

Scheme 12. Kg scale Nickel-catalyzed reductive cross-coupling reaction yielding **39**.

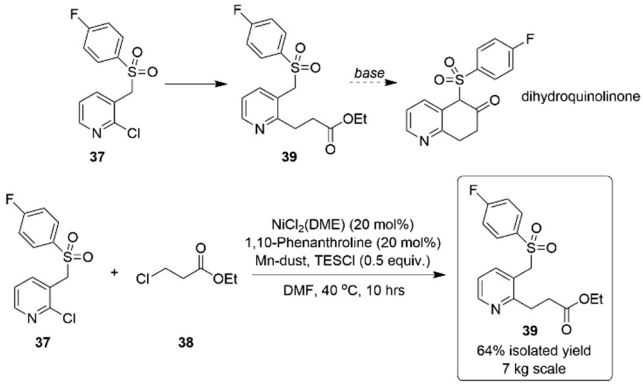

It is worth mentioning that newly revived synthesis methodology, such as photocatalysis and electrocatalysis, has also relied on the application of non-PGM catalysts. [1]

Alcázar and co-workers reported a mg scale nickel-catalyzed Negishi cross-coupling between freshly prepared organozinc derivative **40** and aryl halides **41**. [2] As shown in Scheme 13, the reaction efficiency can be accelerated extensively by visible-light irradiation alone without the addition of any photocatalysts. The reaction was performed using a $NiCl_2$(DME) and dtbbpy catalyst system. For the synthesis of **42a**, the yield of the product differs by as much as 90% with and without light participation. Particularly, light irradiation had a significant effect on the conversion when strongly electron donating groups were present in the molecule, such as in compounds **42b** and **42c**. Notably, as represented by **42d** and **42e**, substrates with electron-withdrawing groups only required 2 mol% of the nickel catalyst. Moreover, as the reaction is carried out in flow, direct scalability could be relatively easily achieved, and the overall approach is superior to batch protocols.

Scheme 13. Nickel-catalyzed Negishi cross-couplings at mg scale.

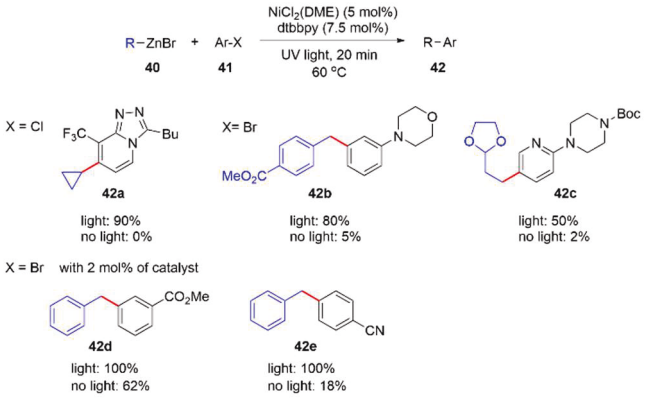

With respect to nickel catalysis combined with electrochemical technique for the purpose of cross-electrophile coupling reactions; a nice review was published recently by Prof. Qiu et al. Nickel-catalyzed reductive couplings for C(sp^2)–C(sp^3) bond formation are becoming well-developed methodologies. Nevertheless, performing these reactions on industrial scale introduces a number of challenges due to the sacrificial stoichiometric metal or amine reductants typically employed. In 2023, a scalable electrochemical approach was demonstrated for the synthesis of pharmaceutically relevant structures. The method utilizes H_2 as the formal reductant in an electrochemical setup by leveraging a cascade of catalytic reactions. The nickel-catalyzed coupling was optimized to 10 mol% $NiBr_2$ trihydrate and a 4:1 ratio of the ligands dtbbpy and ttbtpy. The method was performed on gram scale using an electrochemical flow reactor to obtain core structure **43** found in Rolipram and intermediate **44** in the synthesis of Cenerimod (Scheme 14).

Scheme 14. A scalable electroreductive nickel-catalyzed cross-electrophile coupling of aryl and alkyl bromides.

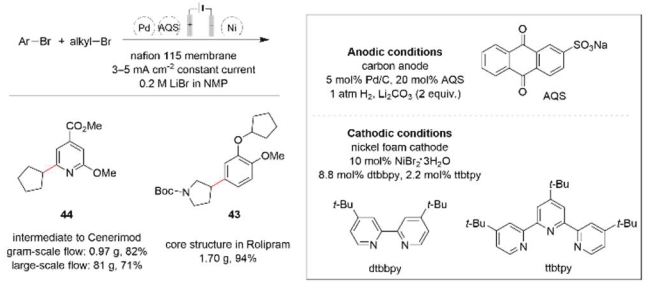

In recent years the advanced bidentate phosphine ligands from the DuPhos and BPE families have also demonstrated utility in non-PGM catalyzed asymmetric hydrogenation reactions. In particular, the Me-DuPhos series has been extensively investigated for non-PGM catalysis in academia during the last decade. As shown in Scheme 15, taking advantage of the coordination chemistry of (*S*,*S*)-Me-DuPhos, Chirik and co-workers developed a highly active and enantioselective phosphine–nickel catalyst for the asymmetric hydrogenation of α,β-unsaturated esters **45**. Reaction screening demonstrated that an air-stable nickel source in combination with Bu_4NI additive as well as Me-DuPhos with a molar ratio of 1:1:1 was the most effective catalytic system in methanol. The reaction was performed at mg scale and tolerated a range of substrates with electron donating and withdrawing functional groups, yielding (*S*)-**46** with up to 99% isolated yield and 96% ee. With the increasing commercial availability of the DuPhos and BPE family of ligands, this is now becoming a methodology worthy of attention for the process chemist.

Scheme 15. Mg scale asymmetric hydrogenation of 45 with a combination of nickel catalyst and Me-DuPhos.[a]

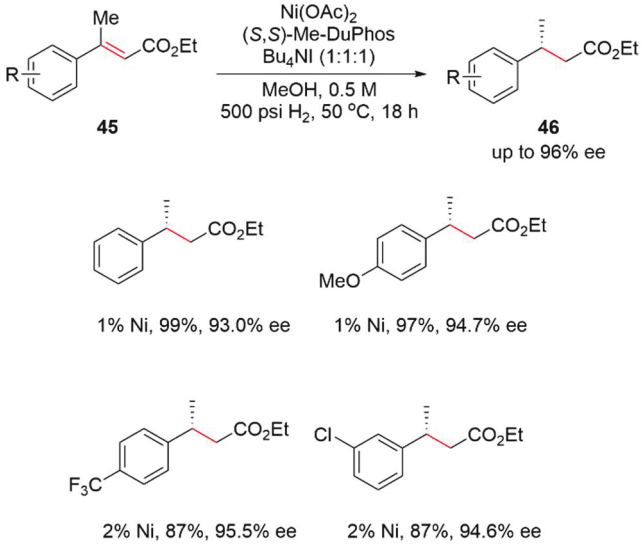

[a] $Ni(OAc)_2$: (*S*,*S*)-Me-DuPhos: Bu_4NI = 1:1:1

2.2 Copper

Copper catalysis is probably the most widely applied alternative to PGM catalysts in the pharmaceutical setting. The foundations of modern copper-catalyzed coupling reactions were established from Ullmann and Goldberg's pioneering research. Since then, numerous copper-catalyzed cross-coupling reactions, especially those conducted under ambient conditions, have been developed in academia to construct C–C and C–heteroatom bonds. Importantly, the discovery of advanced bidentate ligands, such as diamines, 1,3-diketones and oxalic diamides, over the past two decades has extensively expanded the substrate scope of copper catalysis. Ma and co-workers have comprehensively summarized the development of useful reaction conditions for the coupling of (hetero)aryl halides with different nucleophiles. Copper-mediated functionalization of aryl halides was well reviewed by Priyadarshini et al. Furthermore, pyridines and pyrimidines produced via copper catalysis, as well as the market potential and prospects were also systematically reviewed.

The Chan–Lam coupling, the copper-catalyzed C–N or C–O oxidative coupling of organoboron and heteroatom nucleophiles, is an excellent example of a transformation that is well-accepted both among medicinal and process chemists.

Taking advantage of aerobic oxidation, in 2019, scientists at Lilly reported a copper-catalyzed continuous process for multi-kilo scale production of penultimate intermediate of an API (Scheme 16). [1]

Scheme 16. Kg-scale preparation of 4**9** via optimized Cu-Catalyzed Chan–Lam coupling reaction.

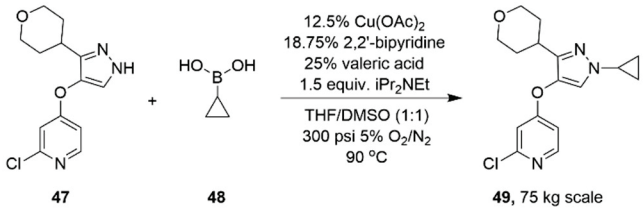

47 **48** **49**, 75 kg scale

The homogeneous reaction mixture of $Cu(OAc)_2$ and bipyridine allowed the reaction to be carried out in a continuous vapor–liquid pipes-in-series reactor. In addition, the development of this oxidative coupling exemplifies a successful strategy for the implementation of aerobic oxidation in pharmaceutical manufacturing. Examples of this type of oxidation are relatively limited in this industry. Partly due to the creation of a potential flammable atmosphere composed of the mixture of oxygen gas and organic solvents. 'Synthetic air' typically consists of less than 10% O_2 in N_2. In 2015, Stahl et al. developed a CuI/ABNO/NMI-catalyzed aerobic alcohol oxidation process. Using this protocol, functionalized primary and secondary alcohols were oxidized to aldehydes and ketones with high efficiency, suitable for use in both batch and flow processes. This catalyst system was demonstrated in a 〉50 g scale batch reaction. [2] Chemists at GSK also reported a 400 g scale aerobic oxidation synthesis of LSD1 inhibitor GSK2879552 (Scheme 17). The starting aliphatic alcohol **50** transformed within 2hrs to the corresponding aldehyde **51** facilitated by the CuI/TEMPO system. The use of sulfolane as a high flash point solvent, low cost catalyst components, and reaction concentration of >0.5 M make this method amenable to safe large-scale application in a batch reactor.

Scheme 17. CuI/TEMPO catalyzed oxidation of alcohol 50 to aldehyde **51** on 400g scale.

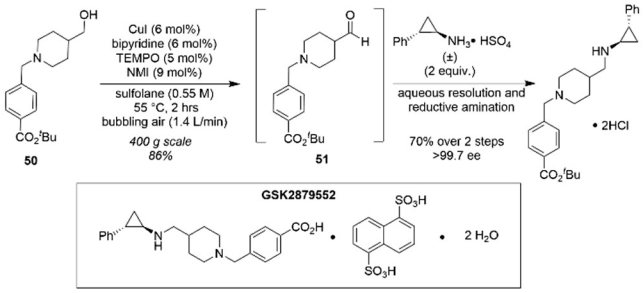

Some work has been done with respect to establishing the limiting oxygen concentrations in a number of common solvents in order for these reactions to be better understood and hopefully more widely employed. One solution that could potentially allow for the safe use of 100% (pure) O_2 is the implementation of continuous flow processes rather than batch reactions, like in the example from the Lilly laboratories. [3] With increasing expertise and improving equipment available, the implementation of more and more flow processes in the pharmaceutical industry is becoming a reality, and perhaps aerobic oxidations are not far away from joining other hazardous reactions that have found a solution in flow.

Another example of copper catalysis developed by a pharmaceutical lab is the large-scale synthesis of AZD8926, a GSK3β inhibitor (Scheme 18). A key step in the scalable route involves the copper-catalyzed dehydrogenative aromatization of the intermediate **53a**. Similarly, it was reported that using oxygen as the stoichiometric oxidant with $Cu(OAc)_2$ as the catalyst is crucial to the success of this route. To remove copper from the product, a solution of 5% NH_3 (aq.) was added (effective removal down to <50 ppm, without ammonia >2500 ppm). The mixture was cooled to 0 °C, precipitating **53** with an HPLC purity of 99% on a 120 g scale.

Scheme 18. Scale up route to AZD8926 via Cu-Catalyzed synthesis of the key intermediate **53.**

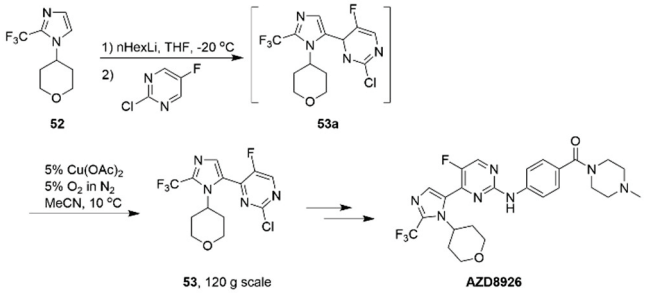

52 **53a** **53**, 120 g scale **AZD8926**

One interesting example of non-PGM application in industry was reported by researchers at Novartis. By means of using a series of novel oxoacetic acid ligands, they developed a copper-catalyzed cross-coupling of DNA-conjugated aryl iodides **54** with aliphatic amines **55**. The air-stable oxoacetic acid ligand **L1** ensured that the transformation proceeded in aqueous DMSO at low temperature and in air. This makes the reaction an ideal methodology candidate for the synthesis of DNA-encoded libraries **56** (Scheme 19).

Scheme 19. Copper-catalyzed amination of DNA-conjugated aryl iodides **54.**

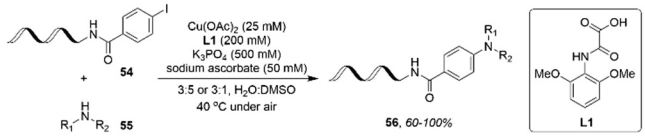

54 **55** **56**, *60-100%* **L1**

Verubecestat (MK-8931), is an inhibitor of β-secretase and it was developed initially for the treatment of Alzheimer's disease. Although its Phase III trials for the treatment of AD turned out to be a failure, more and more research is showing that Verubecestat has positive effects in the treatment of other ailments. As shown in Figure 11, there are two routes for the synthesis of MK-8931. The second-generation route relies on a copper-catalyzed C–N bond formation between **57** and **58** to produce intermediate **59**. High-throughput experiments demonstrated that the combination of 1,2-diamine ligand **L5** and CuI afforded the highest level of reactivity (Scheme 20). A carefully optimized amount of water is important for obtaining the target product, since protodehalogenation of **57** is a significant undesired side reaction of the process. Additionally, solubility of the base, potassium carbonate, is also crucial. It was found that 50 equivalents of water provided the best balance between maximizing reactivity and minimizing protodehalogenation. Under the optimized conditions, the C–N coupling

product **59** was obtained in 80% assay yield at a tens of gram scale and 70% isolated yield after crystallization.

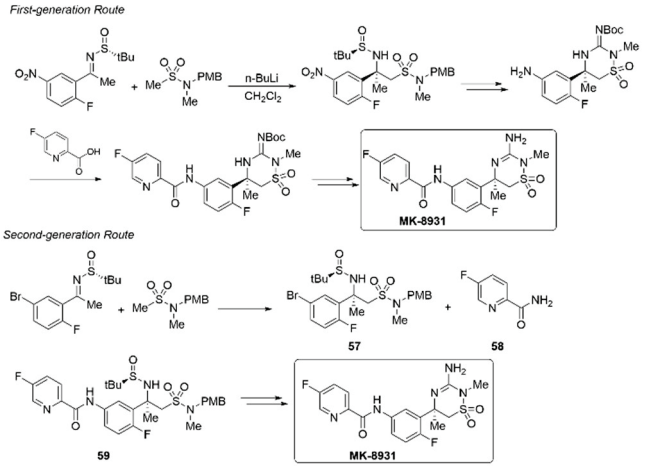

Figure 11. An overview of synthesis of verubecestat MK-8931.

Scheme 20. Tens of gram scale synthesis of intermediate **59** for verubecestat.

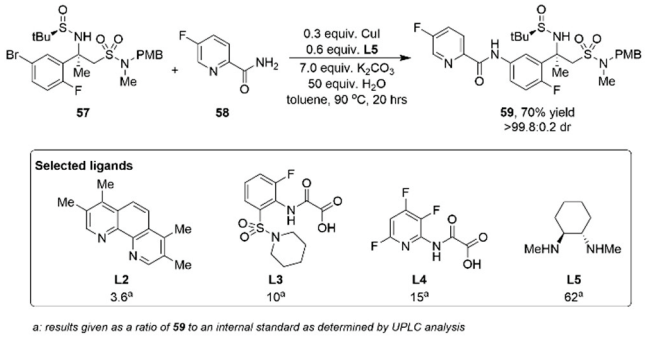

Also, taking advantage of the catalyst system composed of CuI and diamine ligand, recently, a >50 kg scale synthesis route to aminopyrazole building block **63** (Scheme 21) was developed through a collaboration between Pfizer and STA Pharmaceutical. [1] The route proceeds with the amidation reaction of bromide **60** and ammonia surrogate acetamide **61**, followed by acidic hydrolysis of the intermediate **62**, producing **63** in overall 60% yield. Even though the catalyst and ligand loadings are relatively high (12 mol% and 13 mol%, respectively), this procedure provides an alternative to the standard nitration/reduction sequence and avoids energetic intermediates, specialized hydrogenation equipment, and potentially genotoxic impurities that arise from nitro reduction. Residual copper levels were found to be <10 ppm.

Scheme 21. >50 kg scale synthesis of **63** via Cu-catalyzed amidation to provide **62.**

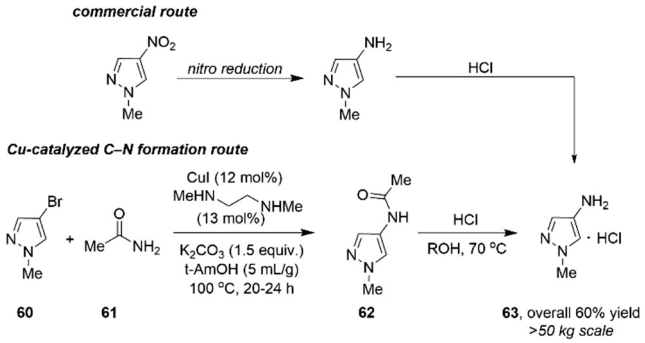

Elbasvir (MK-8742), developed in 2015 through a collaboration between MSD and WuXi Apptec, is a novel small molecule for the treatment of hepatitis C. As shown in Scheme 22, the synthetic challenge of Elbasvir lies in the construction of the central benzoxazinoindole, which contains a hemiaminal ether stereocenter. The route first reported to install the stereocenter proceeds through diastereoselective condensation of indoline **64** with benzaldehyde to yield hemiaminal ether **65**, followed by oxidative aromatization with $KMnO_4$. Although this methodology can deliver indole **66** in 85% yield and >99.2% optical purity, it generates a large amount of insoluble and hazardous MnO_2 waste. Thus, scientists at Merck developed an alternative method for the oxidation step. [2] With a combination of $[Cu(MeCN)_4]BF_4$ as the catalyst and an organic percarbonate TBPC as the stoichiometric oxidant, the reaction proceeds without any by-products and with good conversion and enantioselectivity. The procedure was successfully applied on 500 gram-scale for the synthesis of **66**. To a certain extent, this methodology maximizes product yield and minimizes the environmental footprint of this commonly used synthetic transformation.

Scheme 22. 500 gram-scale synthesis of the key intermediate **66** of Elbasvir.

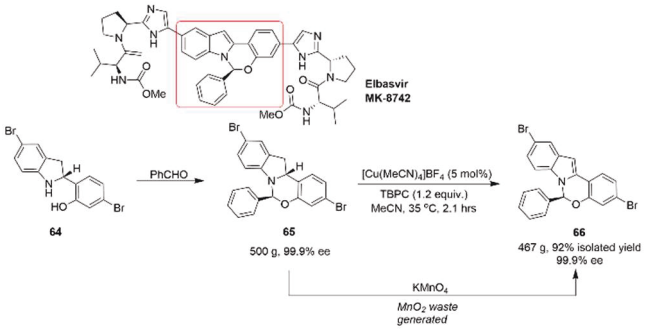

The catalyst loading of any reaction is a very important parameter for the process chemist to consider when choosing a metal catalyst. A high loading of a non-PGM catalyst, just as with a PGM catalyst, will make it difficult to remove metal impurity, which is extremely important for API production. An example representing a balance between the amount of catalyst used and choice of PGM versus non-PGM catalyst is the commercially viable hundreds of kg scale synthesis of the intermediate of BMS-663068 (Figure 12), a HIV attachment inhibitor prodrug. The CuI loading in the C–N coupling step is up to 30 mol%, but the adoption of APDTC as

copper scavenger can decrease the level of residual copper to an acceptable level. An innovative salt metathesis promoted the isolation of **69**, which could be isolated via a facile filtration process thanks to its solid-state properties. The final processing conditions resulted in the isolation of **69** in good yield (66%) with excellent quality (>98 area%, >96 wt%).

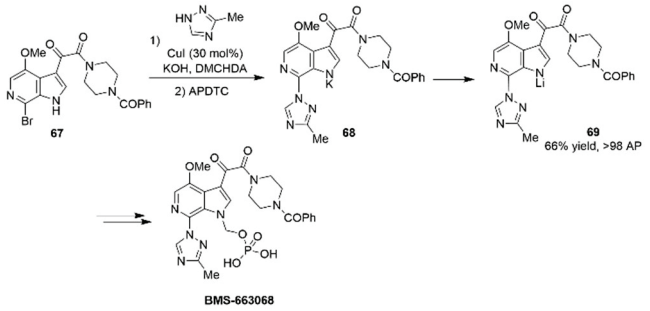

Figure 12. Commercially viable (hundreds of kg scale) synthesis of an intermediate towards BMS-663068 (DMCHDA = dimethylcyclohexane-1,2-diamine; APDTC = ammonium 1-pyrrolidinedithiocarbamate)

Recently, the Roche R&D group described another gram scale copper-catalyzed C–N bond-forming reaction, namely a selective mono-amination reaction of an aryl bromide using gaseous NH_3 (Scheme 23), as part of route scouting to synthesize gemlapodect. Although impressive results were achieved, the toxicity associated with aniline intermediate **71** led the team to develop an alternative route.

Scheme 23. Copper-catalyzed C–N bond formation (gram scale) in the synthesis of gemlapodect.

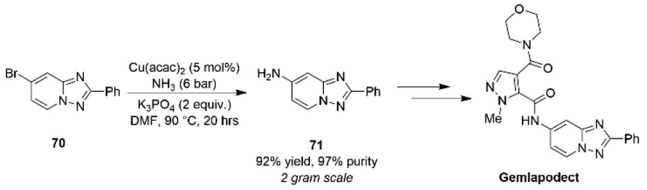

Scheme 24 describes a highly efficient precious-metal-free synthesis of a key tetrahydropyranol intermediate of DPP-4 inhibitor omarigliptin MK-3102. The synthesis of MK-3102 utilizes simple starting material **72** and proceeds in four linear steps. Intermediate **73** was synthesized via an optimized asymmetric Henry reaction that takes advantage of 0.4 mol% of both $CuCl_2$ and **L6** as the catalyst system, affording **73** in 92% yield with 93% ee within 15 hours. The following one-pot nitro-Michael–lactolization–dehydration telescoped process results in **74**. These conditions were successfully demonstrated on kg scale.

Scheme 24. Kg scale practical asymmetric Henry reaction catalyzed by Cu-diamine complex.

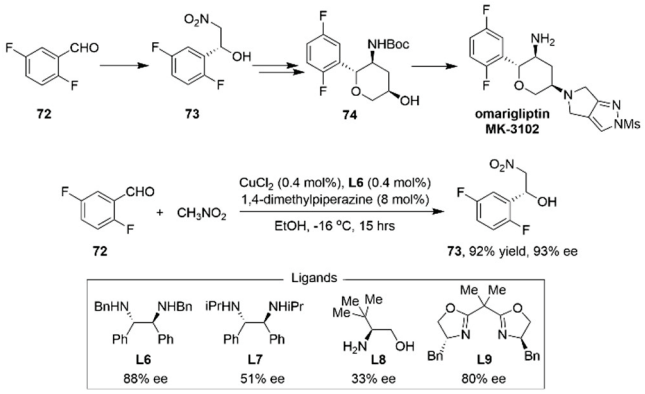

Scientists at Merck leveraged a copper-catalyzed C–O coupling for the synthesis of the important intermediate **77** in the manufacturing process of Gefapixant used in treatment of chronic cough. The authors developed a *para*-bromination protocol of the commodity chemical 2-isopropylphenol **75** which was then efficiently converted to aryl methyl ether **77** using methoxide under copper catalysis (Scheme 25). The purity of **76** had a profound influence on the success of the copper-catalyzed reaction. The authors identified crystallization of **76** with DABCO to provide suitable purity to ensure reproducibility, thereby enhancing the robustness of the methoxylation step. Importantly, these bromophenol-DABCO cocrystals **76** were also found to suppress the formation of an oxidative dimerization byproduct, which otherwise formed when using the unprotected phenol under copper catalysis. The route was performed on 120-kg scale to afford intermediate **77** containing just 11 ppm copper.

Scheme 25. The copper-catalyzed methoxylation of the bromophenol-DABCO cocrystals **76** to provide a robust and cost-efficient process to **77,** an early intermediate in the synthesis of Gefapixant.

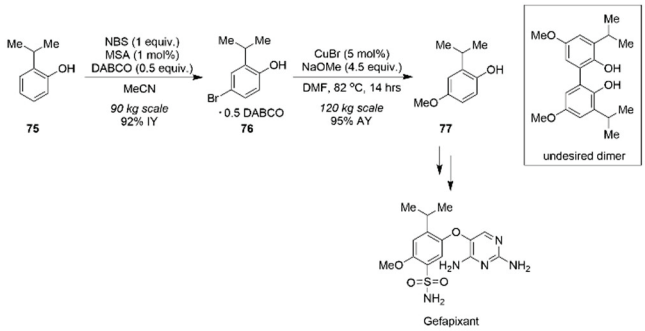

The late-stage introduction of a phenol is important in certain cases due to instability of an intermediate or lack of starting material. Scientists at Merck developed a catalyst system composed of ligand **L10** and CuI salt, with the goal of synthesizing phenols **80** (Scheme 26). Ligand **L10** was found to be the most effective through a combination of high-throughput experimentation, mass-directed ligand library purification and rational ligand evolution. The catalyst system ensured a mild mg scale copper-catalyzed reaction for the synthesis of phenols with a traceless hydroxide surrogate **79**, and therefore enabled the late-stage synthesis of numerous drug-like phenols.

Scheme 26. Late-stage mg scale synthesis of numerous drug-like phenols.

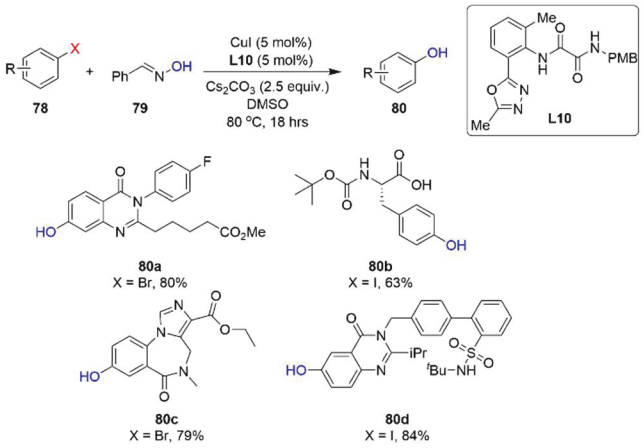

A reaction class where enantioselective copper catalysis has proven to be enabling is the [3+2] cycloaddition, where copper serves as an effective chiral Lewis acid. Researchers at AbbVie developed such a method to access multi-kilograms of the pyrrolidine core of ABBV-3221 (Scheme 27).

Scheme 27. Kg scale Cu(I) catalyzed [3+2] cycloaddition reaction in the synthesis of ABBV-3221.

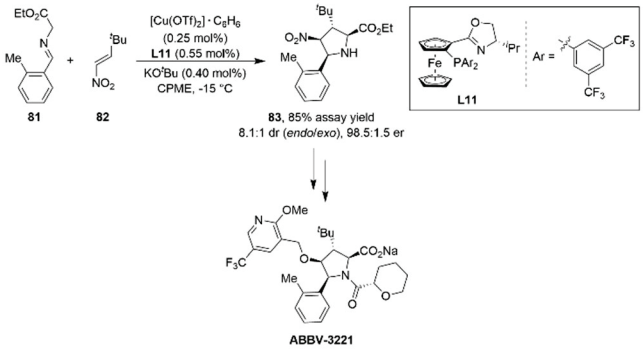

The cycloaddition reaction was found to proceed with the highest stereoselectivity, yield, and reproducibility using the impressively low loading of 0.25 mol% $Cu(OTf)_2 \cdot C_6H_6$ and 0.55 mol% of ligand **L11**. This process was successfully implemented on the pilot plant to produce two 20 kg batches of cycloaddition product **83**. A critically important aspect of the scale-up campaign was controlling the exotherm of the reaction to maintain the high enantioselectivity. This was achieved by diluting the nitro-olefin in CPME as well as increasing the addition time of this reactant from 0.5 to 3.5 hours.

The 2022 Nobel Prize in Chemistry was awarded for the development of click chemistry and bioorthorgonal chemistry. One example of an industrial application of this reaction is in the synthesis of antibody-drug conjugate Trodelvy which was approved by the FDA in 2020. A key step in the synthesis of the appropriate linker between the cytotoxin and the antibody is the copper-catalyzed click reaction (Scheme 28). Employing this copper-catalyzed reaction allowed rapid attachment of the maleimide group **84** before the drug conjugate was attached to the antibody.

Scheme 28. Cu-catalyzed click reaction for the assembly of the linker in ADC Trodelvy at mg scale.

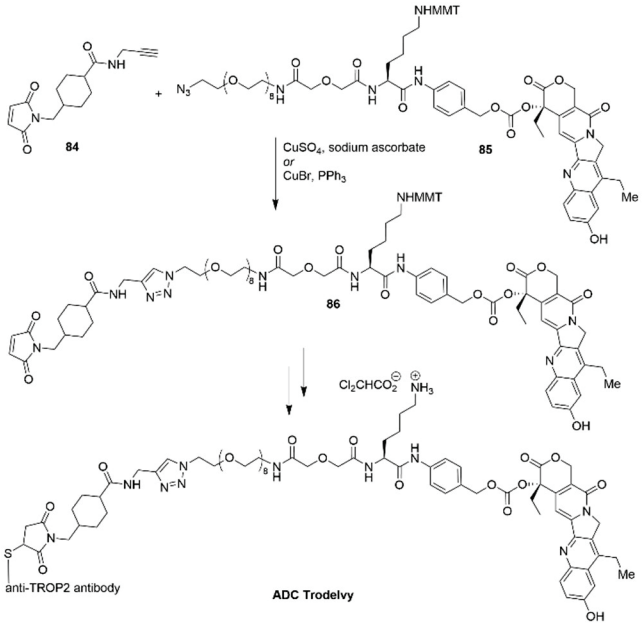

In the agrochemical industry, production scales are typically much greater than those of pharmaceuticals at similar stages of development. Thus, optimized agrochemical processes tend to require very low catalysts loadings when homogenous PGM catalysts are used. Non-PGM catalysts are an attractive alternative, which can obviate the need to develop coupling reactions that proceed with ultra-low palladium loadings (e.g., for C–N couplings). An interesting case study was recently reported by Li and coworkers at Corteva, during development of the manufacturing process for the insecticide tyclopyrazoflor.[1] To form a key pyridine–pyrazole bond, three Ullman couplings were studied (Scheme 29).

Initially, the authors considered an early stage coupling of bromopyridine with an aminopyrazole as part of a proposed route (Scheme 29A). The reaction proceeds effectively with CuCl, since the aminopyrazole can serve as a ligand. Approximately 10% of the regioisomer resulting from coupling at the primary amine was observed, but this impurity could be purged by crystallization. Despite the moderate yield, both starting materials and the catalyst were very economical, and the reaction was viewed as a successful proof of concept.

Next, a second route was developed with a mid-stage Ullman coupling (Scheme 29B). A ligand was required to promote this reaction. The authors successfully performed the reaction on 80 kg scale using DMEDA and CuI. The conditions were further optimized using CuCl in place of CuI to reduce iodide waste and lower the cost. The authors found that L/Cu ratios of 2:1 to 5:1 afforded high conversion at <10 mol % CuCl. Impurities resulting from arylation of the acetamide group were well-controlled during the process and purged during the isolation from DMF/water. These conditions were scaled up to multiple 50 kg batches, affording 70–75% yield of the isolated product in high purity. The authors also considered a later-stage Ullman coupling, such as the reaction shown in Scheme 29C. Here, the reaction yields were significantly lower than the mid-stage Ullman.

As is often the case in pharmaceutical process development, the greater cost of the starting materials going into a late-stage step often means that yield is prioritized over cost of the catalyst.

Ultimately, the route featuring the mid-stage Ullman coupling (Scheme 29C) was selected for further development. This decision was driven by a holistic evaluation of the process cost, safety, and efficiency, though the performance of the copper catalyst played a key role. The low cost, forgiving L/M ratio and facile purge of DMEDA continue to make it a privileged ligand for large-scale Ullman couplings.

Scheme 29. Ullman couplings studied during development of an agrochemical manufacturing process.

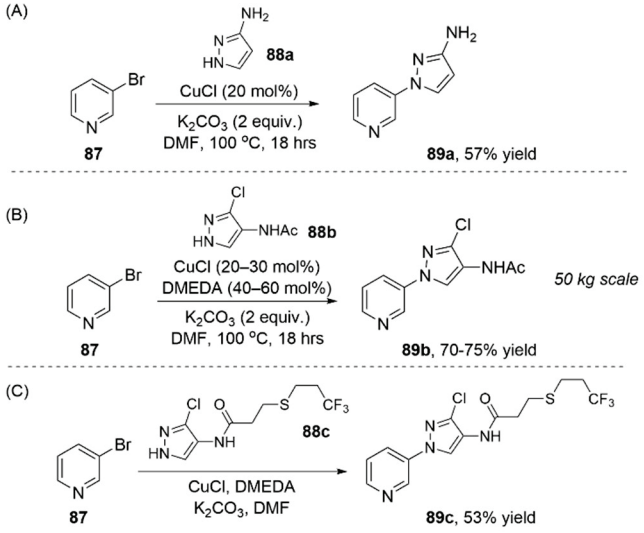

A novel application of copper catalysis for an alternative synthesis of arylated pyrazoles was recently reported by Yu and coworkers at Shenyang Sinochem Agrochemicals.[11] The authors needed to conduct the cyclization of a hydrazine with diethyl maleate to generate a pyrazole precursor for the insecticide tetrachlorantraniliprole **92** but obtained <50% yield under the standard conditions (Scheme 30). They reasoned that previously reported examples of copper- or palladium-catalyzed addition of anilines to activated olefins could be amenable to this reaction.[12] After screening a range of palladium, copper, and nickel complexes, the authors arrived at $(PPh_3)_2CuI$ as the optimal catalyst in terms of activity and cost. This complex provides an impressive rate acceleration at <0.1 mol %. Based on the authors' observations and related literature, it appears that the role of copper is to promote an intramolecular conjugate addition. The reaction was successfully performed on 0.5 mol scale using 0.03 mol% $(PPh_3)_2CuI$, affording the pyrazole precursor **91** in 81% isolated yield. This example serves as a reminder that copper complexes can be cost-effective promoters of challenging conjugate additions.

Scheme 30. Copper-catalyzed cyclization of arylhydrazine **90** with diethyl maleate.

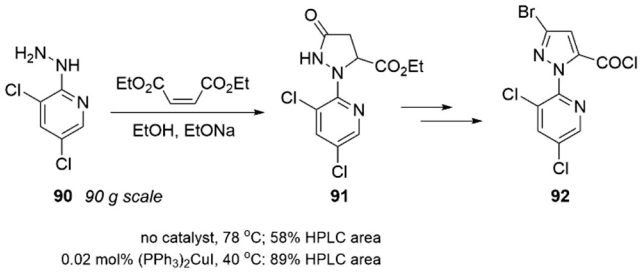

Finally, a reaction that merits discussion although no scale-up efforts can be found in the literature to date, is the copper-catalyzed enantioselective propargylation of aldehydes that was reported by researchers at Boehringer Ingelheim (Scheme 31).[1]

Scheme 31. Copper-catalyzed propargylation of aldehydes **93** at mg scale.

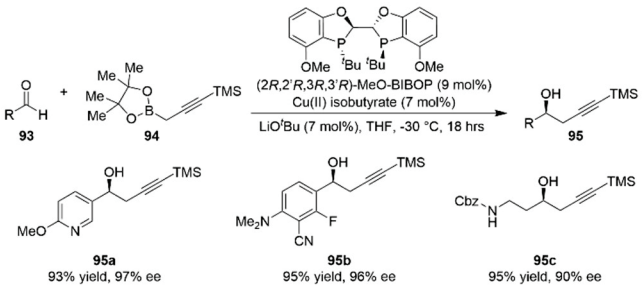

The resulting chiral homopropargylic alcohols (**95**) could be useful intermediates in the synthesis of pharmaceutically interesting compounds due to the pendant alkyne functional group, which can be further derivatized through coupling reactions or other transformations. The team at Boehringer Ingelheim demonstrated a relatively broad substrate scope, using 7 mol% Cu(II) isobutyrate and 9 mol% of the chiral ligand MeO-BIBOP. These numbers would quite likely require optimization to reduce loadings, were this reaction to be scaled up. Nevertheless, it provides a good example to illustrate the capabilities of chiral copper catalysts in assembling versatile enantioenriched building blocks.

2.3 Cobalt

In comparison to the number of applications of nickel and copper catalysis in industry, examples using cobalt catalysis are uncommon. One reason could be the lack of specialized ligands that offer sufficiently high selectivity for the broad assortment of substrates encountered in pharmaceutical research. Another factor could be that the difficulty of removing any cobalt residue from the final product is a concern for large-scale industrial production. While there are well-known sustainability challenges with respect to the scale of cobalt production required for the lithium-ion battery industry, cobalt still remains a more economical alternative to the PGM catalysts for the foreseeable future. Hence, chemists in industry are still paying attention to the field of cobalt catalysis. As early as in 2011, scientists at Merck reported a mild route, using unactivated alkenes as substrates and salen-cobalt complex **B**[1] as the catalyst to synthesize tertiary alkyl/aryl sulfides (**98**) in a regioselective manner (Scheme 32).[1] The reaction works with both electron-

deficient and rich sulfur electrophiles as well as different types of substituted alkenes, resulting in the corresponding alkyl aryl sulfides (**98**) in 70–98% yield. The reaction demonstrated a broad substrate scope; however, no scale-up experiment was reported. Nevertheless, the potential of cobalt catalysis in real-world applications is evident. In 2012, chemists at Hitachi reported a gram-scale cobalt-catalyzed enantioselective borohydride reduction of **99** to **100**, taking advantage of a continuous-flow system (Scheme 33).[1] Because of the intrinsic exothermic features of this reaction, precise temperature control is important for maintaining high enantioselectivity. The use of a microreactor ensured the high temperature required for the reaction was maintained and shortened the residence time to 12 min, thus maintaining the enantioselectivity at 92% ee while keeping the high yield.

Scheme 32. Small scale cobalt-catalyzed synthesis of tertiary alkyl/aryl sulfides **98.**

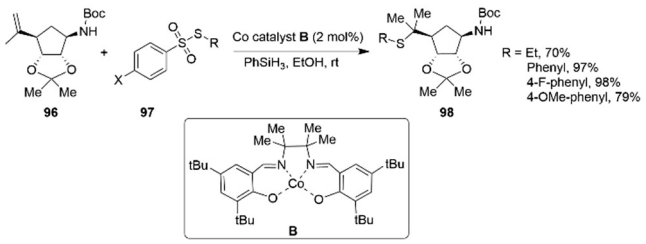

Scheme 33. Cobalt-catalyzed gram-scale borohydride reduction of tetralone derivative **99** under continuous-flow conditions.

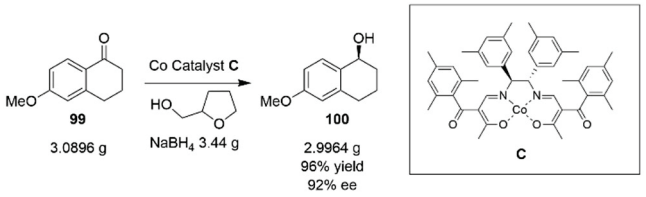

Substrate	Batch		Microreactor	
	yield	ee	yield	ee
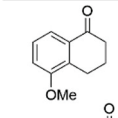	80%	87%	92%	90%
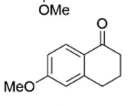	95%	92%	91%	90%
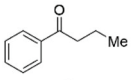	96%	67%	78%	68%
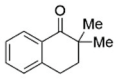	32%	68%	37%	67%

Besides the above mentioned C–S bond formation and borohydride reduction reactions promoted by cobalt, Co-salen catalysts also enable asymmetric cyclopropanation of fused electron-deficient azaheteroarenes.[1] As shown in Scheme 34, Co-salen catalyst **D** promoted the transformation of heteroaromatic derivatives **101** and **102** into the corresponding cyclopropane products **103** and **104**, respectively, with high diastereomeric and enantiomeric ratios up to 99:1 er and 24:1 dr. The cyclopropane derivatives can be further functionalized to provide complex heterocyclic building blocks.

Scheme 34. Cobalt-salen catalyzed mg scale asymmetric cyclopropanation of fused heteroaromatics **101** and **102.**

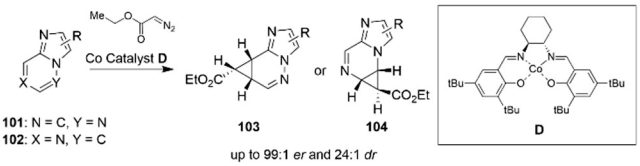

An example of an academic methodology using non-PGMs that was quickly translated into a large-scale process is the cobalt-catalyzed cyclopropanation reported by the Uyeda group.[1] A collaborative team between Pfizer and Curia found the method to provide an intriguing alternative route to key intermediate **107** in the synthesis of the antiviral medication Nirmatrelvir used in treatment of SARS-CoV-2.[1] Applying this methodology allowed the synthesis to start from the readily available and inexpensive material **105** (Scheme 35). Upon optimization, the authors found that employing zinc with an iodine activator circumvented the need for the zinc bromide additive which had originally been reported. Employing ligand **L12**, full conversion of **106** to **107** was achieved, thereby expediting the purification. Detailed studies of the fate of the cobalt catalyst found that the ligand suffers from decomposition under the reaction conditions necessitating a catalyst loading of 15 mol%. These findings point to an opportunity for future improvements in catalyst design. Application of the current catalytic system proceeds on 205 kg scale in 73% yield over two steps and furnished the desired product in high purity.

Scheme 35. Scalable cobalt-catalyzed cyclopropanation of **106** to obtain key intermediate **107** for the synthesis of Nirmatrelvir.

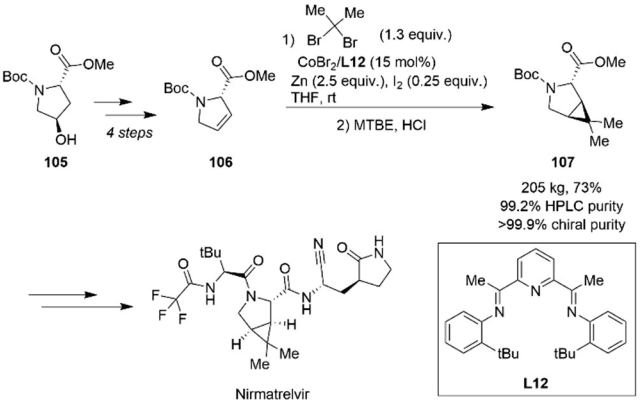

The other ligand that merits discussion with respect to the development of cobalt catalysis is the BPE ligand, which has shown great potential in cobalt-catalyzed asymmetric hydrogenations. One representative example takes advantage of a Zn-mediated activation method to produce hundreds of grams of the epilepsy medication levetiracetam. In 2018, Chirik and co-workers reported the combination of $CoCl_2 \cdot 6H_2O$ and (*R*,*R*)-Ph-BPE exhibited high catalytic activity and enantioselectivity in MeOH for the 200 gram scale asymmetric hydrogenation of dehydro-levetiracetam **108**, affording levetiracetam in 97% isolated yield with 98.2% ee (Scheme 36).[11] Importantly, the catalyst loading in this

catalytic system could be reduced to ~0.08 mol%, lower than the Rh catalyst loading (0.5 mol%) that has been reported.[111] Stoichiometric studies established that the Co(II) catalyst precursor (*R*,*R*)-Ph-BPE$CoCl_2$ undergoes ligand displacement by methanol, and zinc-promoted facile one-electron reduction to Co(I), which coordinated to the bisphosphine ligand more strongly. Another promising use of the Co-BPE catalyst system is in the asymmetric hydrogenation of α,β-unsaturated carboxylic acids **109** and **111** (Scheme 37).[112] The gram-scale synthesis of key intermediates **110** and **112** towards enantioenriched drugs Sacubitril and Artemisinin, respectively, was thus achieved, with the catalyst showing high activity (up to 1,860 TON) and excellent enantioselectivity (up to >99% ee). Furthermore, Co(0)-((*R*,*R*)-Ph-BPE)(COD) has been effectively used for the hydrogenation of α,β-unsaturated carboxylic acids to synthesize chiral carboxylic acids, which are useful precursors to for example Naproxen and (*S*)-Flurbiprofen.[11]

Scheme 36. Gram scale synthesis of epilepsy medication levetiracetam.

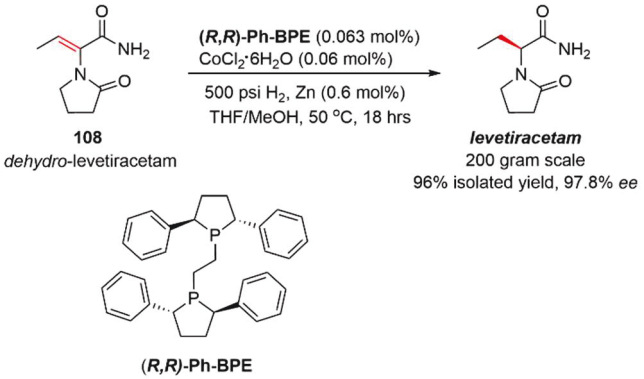

Scheme 37. Synthesis of chiral drug Sacubitril and Artemisinin intermediate **110** and **112** at gram scale.

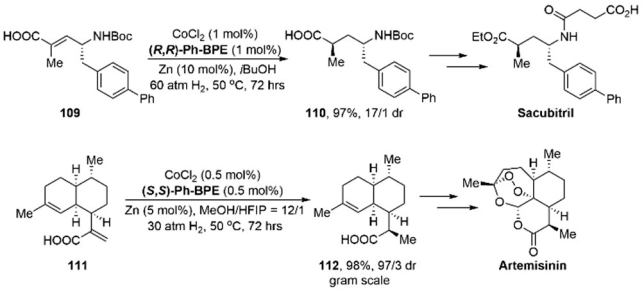

Moreover, cobalt catalysis has also found applications in new fields, as represented by Isayama–Mukaiyama cobalt catalyzed hydroperoxysilylation. This system has now been widely accepted as a superior process for aerobic epoxidation and hydroperoxysilylation of unactivated alkenes.[11] Most recent, Chen and Xue summarized comprehensively the application of cobalt-catalyzed asymmetric reactions in total synthesis of natural terpenoids.[11]

2.4 Iron

Despite being significantly cheaper ($144.90 mt) than other first-row transition metals (Ni: $13.845 lb, Cu: $4.2795 lb, Co: $37.195 lb), applications of homogeneous iron catalysts in industry are relatively sparse.[16] This might be partially due to the instability of iron under catalytic conditions, as it tends to decompose into iron particles as the reaction progresses.[11] In contrast, academic research on homogeneous iron catalysis has been increasing with recent reviews by Nakamura et al.[11] and Ackermann et al. summarizing the state of play in iron-catalyzed C–H bond functionalization reactions.[11] However, most large-scale applications in organic synthesis involving iron-catalysis are iron-catalyzed Kumada cross-coupling reactions, although palladium or nickel catalysts remain the most commonly employed metals in such chemistry. The driver here is most likely a combination of the broad utility of C–C bond-forming reactions in constructing pharmaceutical intermediates and the low toxicity and low cost of iron salts. In 2013, Conlon et al. reported the application of $Fe(acac)_3$ in the multikilogram synthesis of heterocyclic dual NK1/serotonin receptor antagonist **97** (Scheme 38A).[11] The process proceeds through iron(III)-catalyzed Kumada coupling of pyridyl chloride **113** and the corresponding Grignard reagent **114**, followed by benzylic chlorination utilizing trichlorocyanuric acid to selectively construct unsymmetrical 2,4,6-trisubstituted pyridine **115**. This route proved to be highly efficient. Moreover, a commercial kg-scale synthetic route for preparation of cinacalcet hydrochloride **120** (Scheme 38B), a calcimimetic agent and calcium-sensing receptor antagonist, was also described by chemists at Ranbaxy taking advantage of $Fe(acac)_3$/*N*-methyl-2-pyrrolidone (NMP) catalyzed Grignard reaction of alkenyl halide **117** and the Grignard reagent *meta*-(trifluoromethyl)phenylmagnesium bromide (**118**).[12] The synthetic approach involves C–C bond formation to prepare dehydro-cinacalcet (**119**) followed by a hydrogenation reaction.

Scheme 38. Large-scale synthetic routes to **115** and **119** via iron-catalyzed Grignard reactions.

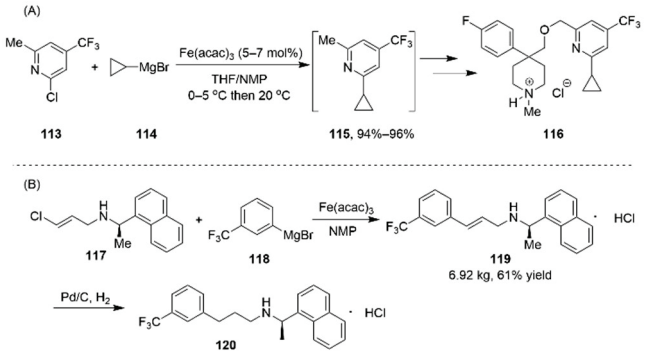

The large-scale synthesis of MCL-509, a potential Parkinson treatment drug, integrates an iron-catalyzed nonclassical Polonovski reaction for the key *N*-demethylation (Scheme 39).[121] This reaction was a great improvement in every aspect over alternative approaches that were explored, including a classical von Braun reaction and chloroformate /hydrazine-mediated demethylation employed in the initial discovery route.

Scheme 39. *N*-Demethylation of MCL-506 Methyl to MCL-509 Amine·HCl.

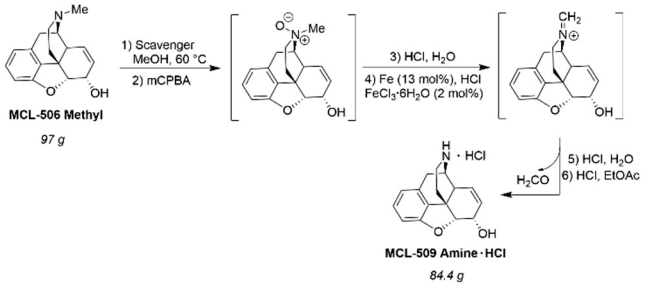

Despite the growing number of successful applications, iron-catalyzed Kumada biaryl cross-coupling reactions still face multiple challenges in industry implementation, including catalyst deactivation, formation of homo-coupling byproducts, limited substrate scope, and intolerance of some functional groups. Chemists at Boehringer Ingelheim developed a continuous flow process that solved these challenges and enabled an iron-catalyzed cross-coupling between 2-chloropyrazine (**121**) and aryl Grignard reagents **122** (Scheme 40).[122] The continuous flow approach overcame the inherent exothermic nature of the reaction, thus enabling longer catalyst lifetime and facilitating scale-up. Moreover, the yield of **123** was significantly improved by up to 30% in continuous flow mode compared to batch mode, and the catalyst loadings was decreased to 0.5 mol%. By utilizing a high-throughput experimentation approach, iron-catalyzed transformation of *ortho*-nitrostyrenes **124** into indoles **125** (Scheme 41) was described by scientists at Merck and University of Illinois at Chicago.[12] The optimal reaction conditions require only 1 mol% of $Fe(OAc)_2$ and 1 mol% of 4,7-$(MeO)_2$Phen with phenylsilane acting as a convenient terminal reductant, producing indole derivatives (**125**) in moderate to high yield. Notably, this is a milder, catalytic, version of the Cadogan-Sundberg indole synthesis which normally utilizes a stoichiometric amount of a trialkyl phosphite as reducing agent.

Scheme 40. Iron-catalyzed Kumada cross-coupling for the synthesis of **123.**

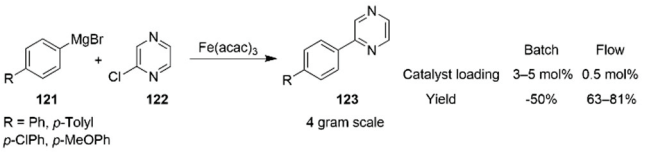

Scheme 41. Mg scale iron-catalyzed transformation of nitrostyrenes **124** to **125.**

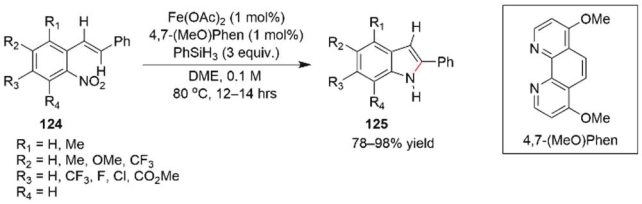

It is worth mentioning that iron catalysts have also shown potential in hydrosilylation reactions. As shown in Scheme 42, in 2012 Chirik et al. reported a series of well-characterized iron complexes containing bis(imino)pyridine ligands (**E**) that promoted the regioselective anti-Markovnikov addition of sterically hindered, tertiary silanes to alkenes under mild conditions.[12] The reaction was performed at mg scale and the iron complex showed high activity and offered broad functional group tolerance. The exclusive regioselectivity limited the formation of undesired stereoisomers to such an extent that the need for separation of unwanted byproducts may not be required in a potential industrial process. Iron is also able to mediate hydrofunctionalization of alkenes by other mechanisms. In particular, iron-catalyzed hydrogen atom transfer (HAT) mediated intramolecular C–C coupling reactions between alkenes and nitriles has also been described.[12] Utilization of $PhSiH_3$ and catalytic $Fe(acac)_3$ introduces a new strategic bond disconnection for ring-closing reactions, forming ketones via imine intermediates.

Scheme 42. Iron-bis(imino)pyridine complex catalyzed hydrosilylation of alkenes at mg scale.

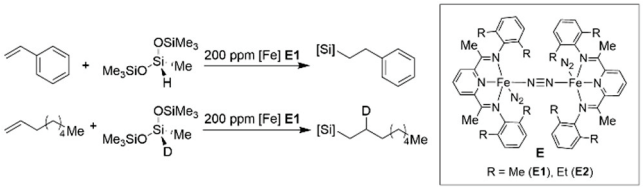

Interestingly, iron-catalysis has also found utility in heterocycle synthesis. A collaboration between the chemists at Janssen and Porton disclosed an efficient synthetic route to quinazolines (a ubiquitous class of compounds displaying a broad range of biological activities) based on iron-catalyzed C(sp^3)–H oxidation and intramolecular C–N bond formation (Scheme 43).[12] Readily available 2-alkylamino benzonitriles (**126**) were used as substrates and reacted with various organometallic reagents to produce 2-alkylamino NH ketimine species (**127**). Taking advantage of $FeCl_2$ as the catalyst and *tert*-BuOOH as the terminal oxidant, C(sp^3)–H oxidation of the alkyl group of **127**, followed by an intramolecular C–N bond formation and aromatization afforded a wide variety of 2,4-disubstituted quinazolines (**128**) in good to excellent yield. The gram-scale synthesis of a series of quinazoline derivatives demonstrated the applicability of this method in organic synthesis.

Scheme 43. Iron-catalyzed synthesis of quinazolines **128.**

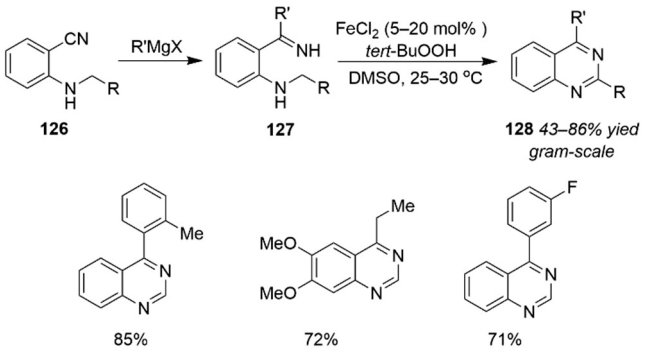

2.5. Manganese

In recent years, manganese catalysts have been explored as alternatives to the more commonly employed PGM catalysts in reactions such as C–H activation, hydrogenation and dehydrogenation reactions.[12,12] Moreover, other reactions

such as manganese-catalyzed three-component reactions of imines/nitriles[12] and intramolecular nitrene transfer reactions have been investigated systematically.[1] However, the application of manganese catalysis in industry is relatively limited. An early example is the application of (dipivaloylmethanato)-manganese(III) ($Mn(dpm)_3$) in olefin hydration, which was initially developed by Mukaiyama et al. in 1990[1] [1] and extended by Magnus in 2000.[1] [2] Since then, the Mn(III)-catalyzed hydration reaction has been broadly accepted as a tool for total synthesis and natural product functionalization.[1] A typical catalytic olefin hydration consists of phenylsilane in isopropanol under dioxygen atmosphere in the presence of $Mn(dpm)_3$ as a catalyst. Specifically, this Mn(III)-catalyzed hydration reaction was employed by chemists at Syngenta in the gram scale synthesis of avermectin derivatives (Scheme 44).[1]

Scheme 44. Manganese-catalyzed olefin hydration reactions for gram scale synthesis of avermectin B derivatives.

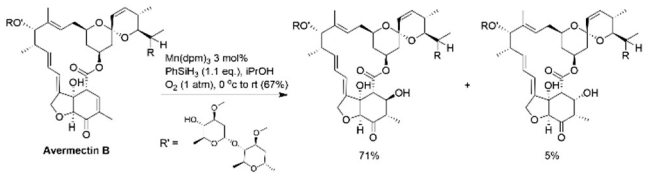

The hydrogenation variant of the Mukaiyama hydration reaction is dubbed metal–hydride atom transfer (MHAT). Manganese-catalyzed hydrogenation and hydrogen transfer reactions have been well reviewed by Sortais et al.[1] In particular, one powerful manifestation of this concept from the Shenvi and Herzon research groups is the manganese- or iron-mediated hydrogenation reduction of C=C bonds.[1] We expect to see future applications of this chemistry in large-scale reactions in due course.

There are isolated examples of the use of manganese catalysts in an industrial setting, for example, the synthesis of aryl-1,3-diones **129** and **130**. The original synthetic route to access **129** was not suited to large-scale synthesis due to the involvement of an aryl lithium intermediate at -78 °C as well as the employment of an aryl lead reagent that is classified as highly toxic. Whilst the aryl-1,3-diones turned out to be promising herbicidal acetyl-CoA carboxylase inhibitors, the successful realization of a kilogram-scale synthesis of these compounds was still uncertain. The solution was found in manganese catalysts by chemists at Syngenta who developed an alternative route employing a manganese-copper catalyzed coupling with alkyl Grignard reagents as the key step to synthesize aryl-1,3-dione motifs **129** and **130** (Scheme 45).[1] The methodology could be applied at kilogram scale for the synthesis of 2-alkyl substituted benzaldehydes and of 2-aryl-1,3-diones.

Scheme 45. Kilogram-scale synthesis of aryl-1,3-dione motifs **129** and **130** via Mn-Cu catalyzed alkyl Grignard coupling.

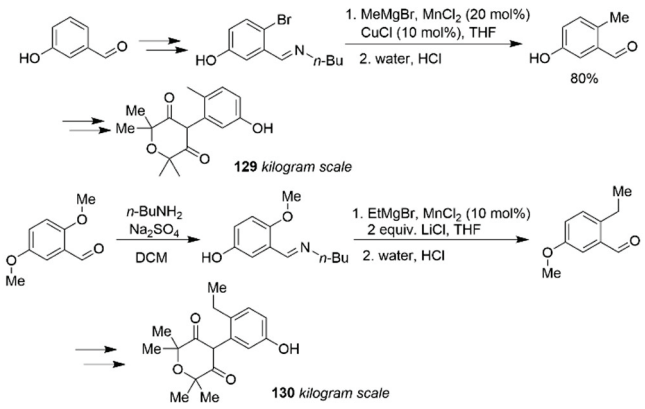

In an effort to leverage the catalytic activity of $Mn_2(CO)_{10}$ in an emerging class of reactions, chemists at Pfizer developed a visible-light-driven Minisci protocol without using precious metal catalysis, such as iridium, ruthenium, or silver.[1] As shown in Scheme 46, this protocol was reported to be compatible with various functional groups, such as sugar moieties (**132a**), spirocycles (**132b**), and others. No peroxide was needed in this photo-mediated Minisci method. Although these reactions were performed at mg scale, the use of a manganese based catalyst provided an economic benefit. This protocol represents an alternative method for functionalization of complex nitrogen-containing drugs, as demonstrated in the case of two representative products (**133**). In this case, late-stage C–H alkylation with either acyclopentyl or isopropyl groups proceeded in 23% and 31% yield, respectively.

Scheme 46. Mg scale manganese-catalyzed photomediated Minisci reaction of quinoline derivatives **131.**

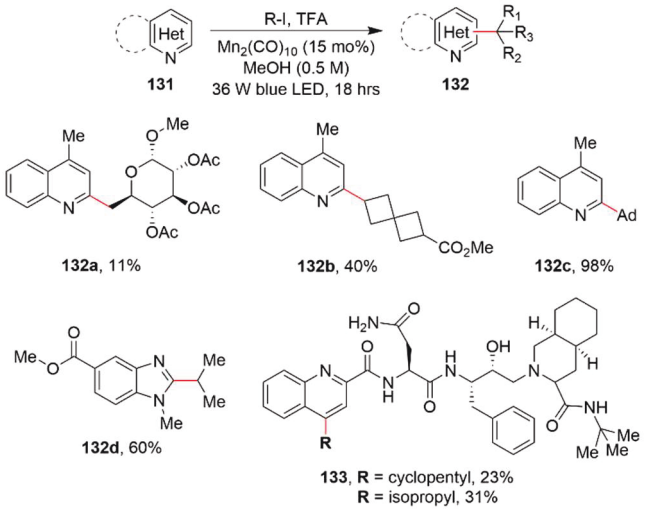

The development of advanced ligands has also fueled the application of manganese catalysts in drug synthesis. Carfilzomib, also known as Kyprolis, is a proteasome inhibitor initially approved by FDA in 2012.[1] According to the public manufacturing routes to Carfilzomib, epoxyketone moiety **136** is a key intermediate. In a recent report by chemists at Amgen, a commercial-scale route to (*S*,*R*)-epoxyketone **136** was disclosed.[1] As shown in Scheme 47, central to this

approach was the development of a kg-scale manganese-catalyzed asymmetric epoxidation method to (*R*,*R*)-epoxyketone **135**, using hydrogen peroxide as the stoichiometric oxidant and (R)-enone **134** as the starting material. Critical to the successful isolation of **136** is a solubility screen identified IPA/water as the ideal crystallization system to reject the undesired diastereomer so that the aid of column chromatography is not required. (*R*,*R*)-Epoxyketone **135** was isolated in 77% yield containing <0.5 % epoxide diastereomer. Epimerization of the leucine side chain in the presence of 20 mol% DBU resulted in (*S*,*R*)-epoxyketone **136**. Subsequently, the kilogram-scale manufacture exploited an analogous NMP/water seeded-batch co-addition crystallization procedure. Eventually, **136** was obtained with ⩾95:5 dr and 98.6 LCAP. This methodology was able to address the challenges associated with the existing bleach epoxidation process and eliminate the requirement for column chromatography.

Scheme 47. Manganese-catalyzed commercial route to intermediate **136** of Carfilzomib.

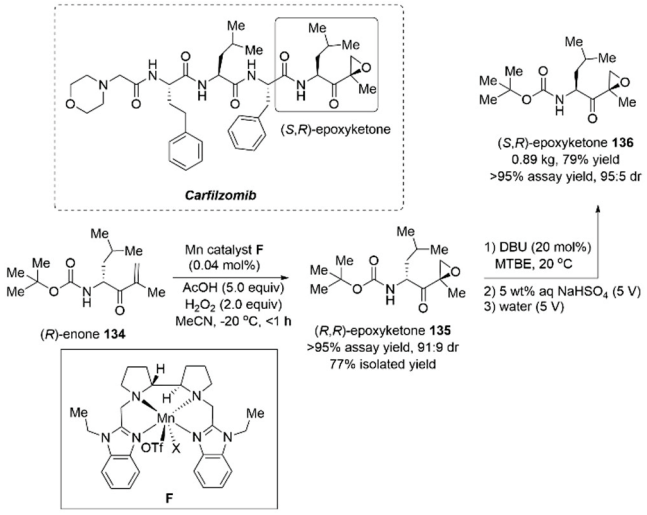

Recently, asymmetric hydrogenation (AH) reactions of unsaturated compounds via manganese-catalysis were also investigated by Liu et al.[1] [1] Through use of chiral NNP-pincer-ligand (L13 or L14) coordinated to manganese, AH of *3H*-indoles with excellent yields and enantioselectivities was achieved (Scheme 48). This methodology expands the scope of AH to substrates which are unsuccessful using a state-of-the-art ruthenium catalyst. The reaction could proceed with catalyst loadings at the ppm level with an exceptional turnover number of up to 72,350. This is the highest value yet reported for an earth-abundant metal-catalyzed AH reaction.[141b]

Scheme 48. Mn-catalyzed decagram-scale asymmetric hydrogenation of *3H*-indole derivatives **137** and **139.**

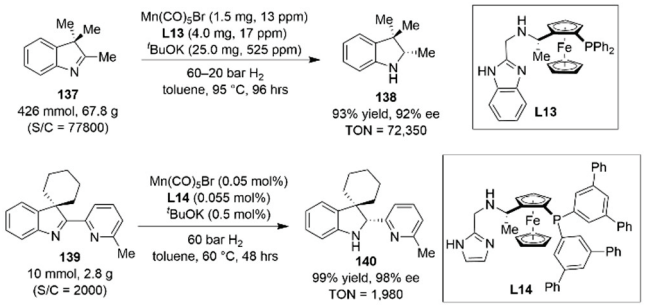

2.6 What about other metals?

In addition to the metals discussed in separate sections above, there are a couple of other non-PGM metals that merit highlighting in this review.

There are several reaction classes for which zinc complexes could be potential catalysts. To mention a few; reduction and oxidation chemistry and carbon dioxide functionalization. A nice perspective article by Enthaler provides a reference for those who may want to read more.[1] [2] However, to the best of our knowledge, the application of zinc catalysts is yet to be reported in large-scale or manufacturing applications. This could be due to many reasons, for example a lack of understanding, and hence control, of the reproducibility of such reactions, or lack of access to the required catalysts in sufficient quantity.

Zinc reagents can not only act as catalysts for certain transformations, but there are also a number of reactions in which they can be useful stoichiometric reagents. One prominent example of this is of course Negishi coupling reactions, where an organozinc species is coupled with an alkyl- or aryl (pseudo)halide. Although this is not the main focus of this article, one specific report by researchers at Pfizer and Snapdragon is nevertheless noteworthy. During the development of a clinical stage active pharmaceutical ingredient, the team identified the zinc complex $[(DMPU)_2Zn(CF_2H)_2]$ as an extremely effective reagent for a selective and high-yielding difluoromethylation reaction. However, they were not able to source this required zinc complex in sufficient quantities to be able to progress the development of this difluoromethylation process. They therefore set out to develop a continuous flow process that could deliver this reagent on larger scale, a task that was successfully accomplished.[1] There are reports of the use of this reagent in nickel or copper catalyzed difluoromethylation reactions,[1] [1] [1] and we eagerly await the authors' coming report on how they subsequently achieved this transformation in their API synthesis project.

Finally, we note that in certain cases the extremely low cost and low toxicity of certain non-PGM compounds can render them highly effective "catalysts" even when they are used in stoichiometric quantities. One such example is the report by scientists at Pfizer of a calcium- or magnesium-promoted amidation of esters with ammonia.[1] A screen of readily available Lewis acids showed that $CaCl_2$ and $Mg(OMe)_2$ were highly effective at promoting this industrially-relevant transformation. The reaction shows remarkable chemoselectivity and can be extended to alkylamines (Scheme 49). A simple aqueous workup was sufficient to remove the

magnesium or calcium salts formed. While reported on small scale in the Pfizer article, these conditions should be readily scalable due to the advantages mentioned above. The use of $Mg(OMe)_2$ for an amidation with dimethylamine was subsequently described on 10 kg scale in a patent (US8680280B2).

Scheme 49. Amidation of esters with ammonia promoted by low-cost and low-toxicity non-PGMs.

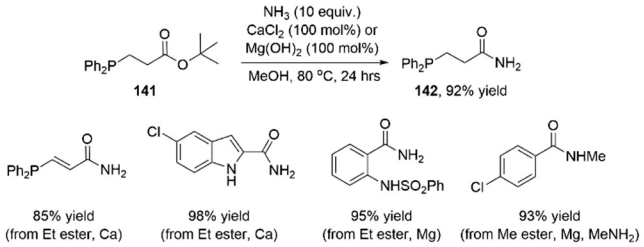

Mg catalysts have been shown to benefit from being used in conjunction with similar ligands to those employed in PGM catalysis.[1] A nice review published by Kwit et al. comprehensively summarized stereoselective transformations that take advantage of magnesium with the advanced ligands employed in PGM catalysis.[1] Several Mg-catalyzed transformations have been reported in small-scale efforts, and we are eagerly on the lookout for applications of these reactions in industry: catalytic hydroboration of alkyl- and aryl-substituted carbodiimides with pinacol borane (HBpin);[1] enantioselective Friedel–Crafts alkylation reactions;[1,1] asymmetric ring-opening reactions[1,2] and chemoselective reduction of α,β-unsaturated carbonyl compounds.[1]

3. CONCLUSION AND OUTLOOK

The number of reaction classes in which non-PGM metals can be employed in place of or in preference to PGMs is undoubtedly on the rise and will keep increasing.

The evaluation of the state of play in non-PGM catalysis reveals several benefits across the entire drug development process, from the delivery of the first few grams to large-scale manufacturing. Non-PGM catalysts can, for example, provide complementary reactivity and substrate scope to their PGM counterparts. However, challenges remain with respect to robustness and reproducibility upon scale-up. For example, nickel catalysts are more prone to substrate inhibition and undesired side reactions, such as protodehalogenation or protodeborylation. Applications of non-PGM catalysis on process scale remain limited in number, most likely due to a combination of factors: a) lack of understanding of reaction mechanism and kinetics of reactions catalyzed by non-PGM as opposed to PGM catalysts; b) reaction conditions that are challenging to scale up (e.g. heterogeneous reaction conditions, carefully control of water stoichiometry); c) lack of commercial availability of the required non-PGM catalysts on the large quantities required. Further collaboration across academic labs, pharmaceutical process development groups, and catalyst and ligand manufacturers is crucial to the successful advancement and introduction of more non-PGM catalyzed processes in large-scale applications. Non-PGM catalysis will most likely never entirely remove the need for PGM catalysts; however, an increasing understanding and evolution within the non-PGM field will ensure that the industrial chemist has a larger number of tractable options available when carrying out route scouting or process optimization.

On writing this article, one extremely important, general, observation shines through the entire story: In addition to the use of more sustainable metal catalysts, the R&D chemist (and indeed R&D managers) would be encouraged to look for solutions from outside of the pharmaceutical field. Non-PGM (base metals as well as first-row transition metals) catalysts have been used on large scale in other industries for many years. We can see a parallel between the earlier adoption of electrochemistry in the fine chemical industry (e.g., the Monsanto adiponitrile process, 1965) and the recent exploration of this technology for pharmaceutical processes.[1] We encourage readers in the pharmaceutical development community to look to other industries (e.g. fine chemicals, material science, polymers) for inspiration in developing new applications of non-PGM catalysis. It is never too late to start, and one never knows what one will find.

AUTHOR INFORMATION

Corresponding Authors

Carin Johansson Seechurn – Sinocompound UK, 14b Warwick Road, Barnet, EN5 5EQ, UK; https://orcid.org/0000-0002-1011-9764; E-mail: carin.seechurn@sinocompound.com

Keary Engle - Department of Chemistry, The Scripps Research Institute, 10550 North Torrey Pines Road, La Jolla, CA 92037, USA; https://orcid.org/0000-0003-2767-6556; E-mail: keary@scripps.edu

Michael C. Haibach - Process Research and Development, AbbVie Inc., 1 North Waukegan Road, North Chicago, Illinois 60064, USA. E-mail: Michael.haibach@abbvie.com

Authors

Anne Ravn - Department of Chemistry, The Scripps Research Institute, 10550 North Torrey Pines Road, La Jolla, CA 92037, USA. https://orcid.org/0000-0002-7040-3230.

Hui Zhao - Sinocompound Catalysts, Building C, Bonded Area Technology Innovation Zone, Zhangjiagang, Jiangsu 215634, China.

Author Contributions

The manuscript was written through contributions of all authors.

ACKNOWLEDGMENT

We thank the Independent Research Fund Denmark (grant ID: 10.46540/3102-00009B) for financial support (A.K.R.). We also thank Richard Qi (Sinocompound CEO), Gerard Compagnoni (Sinocompound COO), Zheng Wang (President) and Juan Li (R&D Director) for useful discussions and support (H.Z. and C.C.C.J.S.)

REFERENCES

(1) Hoppert, M. *Metalloenzymes*, Encyclopedia of Geobiology, 2011, ISBN: 978-1-4020-9211-4, 558-563.

(2) Crawley, M. L.; Trost, B. M. Applications of Transition Metal Catalysis in Drug Discovery and Development: An Industrial Perspective, **2012** John Wiley & Sons, Inc, Weinheim.

( ) J. Seechurn, C. C. C.; Kitching, M. O.; Colacot, T. J.; Snieckus, V. Palladium-Catalyzed Cross-Coupling: A Historical Contextual Perspective to the 2010 Nobel Prize. *Angew. Chem. Int. Ed.* **2012**, *51* (21), 5062-5085.

( ) Chirik, P.; Morris, R., Eds. *Acc. Chem. Res.* **2015**, *48*, 2495, 2576, 2587, 2599, 2612. 10.1021/acs.accounts.5b00385.

( ) (a) Magano, J.; Monfette, S. Development of an Air-Stable, Broadly Applicable Nickel Source for Nickel-Catalyzed Cross-Coupling. *ACS Catal.* **2015**, *5* (5), 3120-3123. (b) Malhotra, S.; Seng, P. S.; Koenig, S. G.; Deese, A. J.; Ford, K. A. Chemoselective sp^2-sp^3 Cross-Couplings: Iron-Catalyzed Alkyl Transfer to Dihaloaromatics. *Org. Lett.* **2013**, *15* (14), 3698-3701.

( ) (a) Lagaditis, P. O.; Sues, P. E.; Sonnenberg, J. F.; Wan, K. Y.; Lough, A. J.; Morris, R. H. Iron(II) Complexes Containing Unsymmetrical P-N-P' Pincer Ligands for the Catalytic Asymmetric Hydrogenation of Ketones and Imines. *J. Am. Chem. Soc.* **2014**, *136* (4), 1367-1380. (b) Friedfeld, M. R.; Shevlin, M.; Hoyt, J. M.; Krska, S. W.; Tudge, M. T.; Chirik, P. J. Cobalt Precursors for High-Throughput Discovery of Base Metal Asymmetric Alkene Hydrogenation Catalysts. *Science* **2013**, *342* (6162), 1076-1080.

( ) (a) Greene, J. F.; Hoover, J. M.; Mannel, D. S.; Root, T. W.; Stahl, S. S. Continuous-Flow Aerobic Oxidation of Primary Alcohols with a Copper(I)/TEMPO Catalyst. *Org. Process Res. Dev.* **2013**, *17* (10), 1247-1251. (b) Liu, J.; Ma, S. Iron-Catalyzed Aerobic Oxidation of Allylic Alcohols: The Issue of C=C Bond Isomerization. *Org. Lett.* **2013**, *15* (20), 5150-5153.

( ) (a) Evans, R. W.; Zbieg, J. R.; Zhu, S.; Li, W.; MacMillan, D. W. C. Simple Catalytic Mechanism for the Direct Coupling of α-Carbonyls with Functionalized Amines: A One-Step Synthesis of Plavix. *J. Am. Chem. Soc.* **2013**, *135*, 16074-16077. (b) Zhu, S.; Niljianskul, N.; Buchwald, S. L. Enantio- and Regioselective CuH-Catalyzed Hydroamination of Alkenes. *J. Am. Chem. Soc*. **2013**, *135* (42), 15746-15749.

( ) (a) Murayama, H.; Nagao, K.; Ohmiya, H.; Sawamura, M. Copper(I)-Catalyzed Intramolecular Hydroalkoxylation of Unactivated Alkenes. *Org. Lett.* **2015**, *17* (9), 2039-2041. (b) Gazzola, S.; Beccalli, E. M.; Borelli, T.; Castellano, C.; Chiacchio, M. A.; Diamante, D.; Broggini, G. Copper(II)-Catalyzed Alkoxyhalogenation of Alkynyl Ureas and Amides as a Route to Haloalkylidene-Substituted Heterocycles. *J. Org. Chem.* **2015**, *80* (14), 7226-7234.

(1) (a) Wang, P.; Yeo, X. L.; Loh, T. P. Copper-Catalyzed Highly Regioselective Silylcupration of Terminal Alkynes to Form α-Vinylsilanes. *J. Am. Chem. Soc*. **2011**, *133* (5), 1254-1256. (b) Wu, J. Y.; Stanzl, B. N.; Ritter, T. A Strategy for the Synthesis of Well-Defined Iron Catalysts and Application to Regioselective Diene Hydrosilylation. *J. Am. Chem. Soc.* **2010**, *132* (38), 13214-13216.

(11) (a) Sirois, J. J.; Davis, R.; DeBoef, B. Iron-Catalyzed Arylation of Heterocycles via Directed C–H Bond Activation. *Org. Lett*. **2014**, *16* (3), 868-871. (b) Chen, Q.; Ilies, L.; Nakamura, E. Cobalt-Catalyzed ortho-Alkylation of Secondary Benzamide with Alkyl Chloride through Directed C-H Bond Activation. *J. Am. Chem. Soc.* **2011**, *133* (3), 428-429.

(12) Sources: (a) https://www.moneymetals.com/copper-prices, accessed on Nov 24, 2023; (b) https://www.dailymetalprice.com/metalpricecharts.php?c=ir&u=oz&d=120, accessed on Nov 24, 2023; (c) https://tradingeconomics.com/commodity/nickel, accessed on Nov 24, 2023; (d) https://matthey.com/products-and-markets/pgms-and-circularity/pgm-management, accessed on Nov 24, 2023.

(1) Ganesan, M.; Krogman, J. P.; Konovalova, T.; Diaz, L. L.; Hsu, C. W. Recent Advances in Sustainable Catalysts and Catalysis with Non-noble Metals. *ChemRxiv* **2023**, doi: 10.26434/chemrxiv-2023-v30kj-v2.

(1) Several examples of this scenario have emerged over the years: (a) 'Amine'-catalyzed Suzuki-Miyaura type coupling reaction: Xu, L.; Liu, F. Y.; Zhang, Q.; Chang, W. J.; Liu, Z. L.; Lv, Y.; Yu, H. Z.; Xu, J.; Dai, J. J.; Xu, H. J. The amine-catalysed Suzuki–Miyaura-type coupling of aryl halides and arylboronic acids. *Nat Catal.* **2021**, *4*, 71-78. (b) 'Iron'-catalyzed cross-coupling: Buchwald, S. L.; Bolm, C. On the Role of Metal Contaminants in Catalyses with $FeCl_3$. *Angew. Chem*. **2009**, *121* (31), 5694-5695. (c) 'Transition-metal free' Suzuki type coupling: Arvela, R, K.; Leadbeater, N. E.; Sangi, M. S.; Williams, V. A.; Granados, P.; Singer, R. D. A Reassessment of the Transition-Metal Free Suzuki-Type Coupling Methodology. *J. Org. Chem.* **2005**, *70* (1), 161-168.

(1) (a) Singer, R. A.; Monfette, S.; Bernhardson, D. J.; Tcyrulnikov, S.; Hansen, E. C. Recent Advances in Nonprecious Metal Catalysis. *Org. Process Res. Dev.* **2020**, *24 (6)*, 909-915. (b) Haibach, M. C.; Ickes, A. R.; Wilders, A. M.; Shekhar, S. Recent Advances in Nonprecious Metal Catalysis. *Org. Process Res. Dev.* **2020**, *24* (11), 2428-2444. (c) Buono, F.; Nguyen, T.; Qu, B.; Wu, H.; Haddad, N. Recent Advances in Nonprecious Metal Catalysis. *Org. Process Res. Dev.* **2021**, *25* (7), 1471-1495.

(1) Piontek, A.; Bisz, E.; Szostak, M. Iron-Catalyzed Cross-Couplings in the Synthesis of Pharmaceuticals: In Pursuit of Sustainability. *Angew. Chem. Int. Ed.* **2018**, *57*, 11116-11128.

(1) Boit, T. B.; Bulger, A. S.; Dander, J. E.; Garg, N. K. Activation of C-O and C-N Bonds Using Non-Precious-Metal Catalysis. *ACS Catal.* **2020**, *10* (20), 12109-12126.

(18) (a) Garg, N. K.; Quasdorf, K. W.; Tian, X. Cross-coupling of phenolic derivatives. US 8,546,607 B2, October 1, 2013. (b) Garg, N. K.; Ramgren, S. D.; Silberstein, A. L.; Quasdorf, K. W. Amination of aryl alcohol derivatives. US 9,567,307 B2, February 14, 2017.

(1) (a) Luescher, M. U.; Gallou, F.; Lipshutz, B. H. The impact of earth-abundant metals as a replacement for Pd in cross coupling reactions. *ChemRxiv* **2024**, doi: 10.26434/chemrxiv-2024-tc9hm (b) Barbu, B. The elements of a green catalyst. *C&EN News* **2024**, *102* (5), cover story. (c) Clapson, M. L.; Durfy, C. S.; Facchinato, D.; Drover, M. W. Base metal chemistry and catalysis. *Cell Reports Physical Science* **2023**, *4* (9), 101548-101574. (d) Wheelhouse, K. M. P.; Webster, R. L.; Beutner, G. L. Advances and Applications in Catalysis with Earth-Abundant Metals. *Org. Process Res. Dev.* **2023**, *27* (7), 1157-1159.

(2) (a) Wang, Z.; Hellweg, S. First Steps Toward Sustainable Circular Uses of Chemicals: Advancing the Assessment and Management Paradigm. *ACS Sustainable Chem. Eng*. **2021**, *9* (20), 6939-6951. (b) https://www.unep.org/topics/chemicals-and-pollution-action/circularity-sectors/green-and-sustainable-chemistry, accessed on April 24, 2024.

(21) Mutlu, H.; Barner, L. Getting the Terms Right: Green, Sustainable, or Circular Chemistry? *Macromol. Chem. Phys.* **2022**, *223*, 2200111.

(22) Nuss, P.; Eckelman, M. J. Life Cycle Assessment of Metals: A Scientific Synthesis. *PLoS ONE* **2014**, *9* (7), e101298. doi: 10.1371/journal.pone.0101298.

(23) Haynes, W. M (Ed.) Abundance of elements in the earth's crust and in the sea, CRC Handbook of Chemistry and Physics, 97th edition **2016–2017**, 14-17, CRC Press, Boca Raton.

(24) https://www.rsc.org/periodic-table/, accessed on Feb 23, 2024.

(2) https://www.statista.com/statistics/273647/global-mine-production-of-palladium/#:~:text=Regional%20palladium%20production,%2C%20North%20America%2C%20and%20Europe.%20Accessed%20on%20December%2020,%202023. Accessed on December 20, 2023.

(2) https://www.woodmac.com/news/opinion/why-iridium-could-put-a-damper-on-the-green-hydrogen-boom/#:~:text=And%20although%20iridium%20has%20a,about%207%20tons%20per%20year. Accessed December 20, 2023.
(2) https://www.mining-technology.com/features/five-most-expensive-metals-and-where-they-are-mined/?cf-view&cf-closed. Accessed on December 20, 2023.
(2) Loferski, P. J.; Ghalayini, Z. T. and Singerling, S. A. (2018) Platinum-group metals. 2016 Minerals Yearbook. USGS. p. 57.3.
(2) https://www.visualcapitalist.com/all-the-metals-we-mined-in-2021-visualized/#:~:text=Industrial%20metals%20are%20largely%20used,million%20tonnes%20of%20these%20metals.&text=*Represents%20refinery%2Fsmelter%20production.,industrial%20metal%20production%20in%202021. Accessed on December 20, 2023.
( ) (a) Anastas, P. T.; Warner, J. C. Green Chemistry: Theory and Practice, Oxford University Press: New York, **1998** (b) For a useful platform of relevant references to each of the 12 principles, see: https://www.acs.org/greenchemistry/principles/12-principles-of-green-chemistry.html, accessed on April 24, 2024.
(1) Clapson, M.L.; Durfy, C. S.; Facchinato, D.; Drover, M. W. Base metal chemistry and catalysis. *Cell Reports Physical Science*, 2023, *4* (9), 101548.
(2) Kettler, P. B. Platinum Group Metals in Catalysis: Fabrication of Catalysts and Catalyst Precursors. *Org. Proc. Res. Dev.* **2003**, *7* (3), 342-354.
( ) For some more in-depth articles on this topic, see: (a) de Faria, D. R. G.; de Medeiros, J. L.; Araújo, Q. Q. F. Sustainability assessment for the chemical industry: Onwards to integrated system analysis. *J. Clean. Prod.* **2021**, *278*, 123966. (b) McCarthy, S.; Braddock, D. C.; Wilton-Ely, J. D. E. T. Strategies for sustainable palladium catalysis. *Coord. Chem. Rev*. **2021**, *442*, 213925.
(34) Egorova, K. S.; Ananikov, V. P. Toxicity of Metal Compounds: Knowledge and Myths. *Organometallics* **2017**, *36* (21), 4071-4090.
(35) Egorova, K. S.; Ananikov, V. P. Which Metals are Green for Catalysis? Comparison of the Toxicities of Ni, Cu, Fe, Pd, Pt, Rh, and Au Salts. *Angew. Chem. Int. Ed.* **2016**, *55* (40), 12150-12162.
(36) U.S. Pharmacopeia National Formulary, First Supplement to USP 40–NF 35, The United States Pharmacopeial Convention, 2017, p. 8065.
( ) Chirik, P. J.; Engle, K. M.; Simmons, E. M.; Wisniewski, S. R. Collaboration as a Key to Advance Capabilities for Earth-Abundant Metal Catalysis. *Org. Process Res. Dev.* **2023**, *27* (7), 1160-1184.
( )Laue, W.; Thiemann, M.; Scheibler, E.; Wiegand, K. W. Nitrates and Nitrites. In Ullmann's Encyclopedia of Industrial Chemistry, Wiley-VCH, Weinheim, **2000**, doi: 10.1002/14356007.a17_265..
( ) Peoples, M. B.; Nielsen, H. H.; Elie, O. H.; Jensen, E. S.; Justes, E.; Williams, M. *Chapter 8 - The Contributions of Legumes to Reducing the Environmental Risk of Agricultural Production*, *Agroecosystem Diversity*, Academic Press, **2019**, Pages 123-143, ISBN 9780128110508.
( ) Elliott, D. C. Biomass, Chemicals from. In Encyclopedia of Energy, Elsevier B.V., Amsterdam, **2004**, *1*, 163-174.
(1) Baraj, E.; Ciahotný, K.; Hlinčík, T. The water gas shift reaction: Catalysts and reaction mechanism. *Fuel*, **2021**, *288*, 119817.
(2) Tolman, C. A.; McKinney, R. J.; Seidel, W. C.; Druliner, J. D.; Stevens, W. R. Homogeneous Nickel-Catalyzed Olefin Hydrocyanation. *Advances in Catalysis*, **1985**, *33*, 1-46.
( ) Kranenburg, M. P.; Kamer, C. J.; van Leeuwen, P. W. N. M.; Vogt, D.; Keim, W. Effect of the bite angle of diphosphine ligands on activity and selectivity in the nickel-catalysed hydrocyanation of styrene. *J. Chem. Soc., Chem. Commun.,* **1995**, 2177-2178.
( ) Goertz, W.; Kamer, P. C. J.; van Leeuwen, P. W. N. M.; Vogt, D. Application of chelating diphosphine ligands in the nickel-catalysed hydrocyanation of alk-l-enes and ω-unsaturated fatty acid esters. *Chem. Commun*. **1997**, 1521-1522.
(Mol, J. C. Industrial applications of olefin metathesis. Journal of Molecular Catalysis A: Chemical 2004, *213* (1) 39-45.
( ) Keim, W. Oligomerization of Ethylene to α-Olefins: Discovery and Development of the Shell Higher Olefin Process (SHOP). *Angew. Chem. Int. Ed.* **2013**, *52* (48), 12492-12496.
( ) Resconi, L.; Cavallo, L.; Fait, A.; Piemontesi, F. *Chem. Rev*. Selectivity in Propene Polymerization with Metallocene Catalysts. **2000**, *100* (4), 1253-1346.
( ) Meiswinkel, A.; Woehl, A.; Mueller, W.; Boelt, H. V.; Mosa, F. M.; Al-Hazmi, A. Developing Linear-alpha-Olefins Technology – From Laboratory to a Commercial Plant. *Oil Gas Eur. Mag.* **2012**, *2*, 103-106.
( ) Olivier-Bourbigou, H.; Forestiere, A.; Saussine, L.; Magna, L.; Favre, F.; Hugues, F. Olefin oligomerization for the production of fuels and petrochemicals. *Oil Gas Eur. Mag.* **2010**, *36* (2), 97-102.
( ) Yang, B.; He, J.; Zhang, G.; Guo, J. *Chapter 15 - Vanadium catalysts*, *Vanadium*, Elsevier, **2021**, Pages 415-443, ISBN 9780128188989.
(1) Nadeina, K. A.; Klimov, O. V.; Pereima, V. Y.; Koryakina, G. I.; Danilova, I. G.; Prosvirin, I. P.; Gerasimov, E. Y.; Yegizariyan, A. M.; Noskov, A. S. Catalysts based on amorphous aluminosilicates for selective hydrotreating of FCC gasoline to produce Euro-5 gasoline with minimum octane number loss. *Catal.Today*, **2016**, *271*, 4-15.
(2) González-Marcos, M. P.; Fuentes-Ordóñez, E. G.; Salbidegoitia, J. A.; González-Velasco, J. R. Optimization of Supports in Bifunctional Supported Pt Catalysts for Polystyrene Hydrocracking to Liquid Fuels. *Top Catal* **2021**, *64*, 224-242.
( ) Franke, R.; Selent, D.; Börner, A. Applied Hydroformylation. *Chem. Rev*. **2012**, *112* (11), 5675-5732.
( ) Jaouen, F.; Proietti, E.; Lefèvre, M.; Chenitz, R.; Dodelet, J. P.; Wu, G.; Chung, H. T.; Johnston, C. M.; Zelenay, P. Recent advances in non-precious metal catalysis for oxygen-reduction reaction in polymer electrolyte fuelcells. *Energy Environ. Sci.*, **2011**, *4*, 114-130.
( ) (a) Percec, V.; Bae, J. Y.; Hill, D. H. Aryl Mesylates in Metal Catalyzed Homocoupling and Cross-Coupling Reactions. 2. Suzuki-Type Nickel-Catalyzed Cross-Coupling of Aryl Arenesulfonates and Aryl Mesylates with Arylboronic Acids. *J. Org. Chem*. **1995**, *60* (4), 1060-1065; (b) Saito, S.; Sakai, M.; Miyaura, N. A synthesis of biaryls via nickel(0)-catalyzed cross-coupling reaction of chloroarenes with phenylboronic acids. *Tetrahedron Lett.* **1996**, 37 (17), 2993–2996.
( ) Dawson, D. D.; Jarvo, E. R. Stereospecific Nickel-Catalyzed Cross-Coupling Reactions of Benzylic Ethers with Isotopically-Labeled Grignard Reagents. *Org. Process Res. Dev*. **2015**, *19* (10), 1356-1359.
( ) (a) Weires, N. A.; Baker, E. L. Garg, N. K. Nickel-catalysed Suzuki–Miyaura coupling of amides. *Nat. Chem*. **2016**, *8*, 75-79.
( ) Cann, R. O.; Waltermire, R. E.; Chung, J.; Oberholzer, M.; Kasparec, J.; Ye, Y. K.; Wethman, R. Process Development for a Large Scale Stereoselective Synthesis of (Z)-(1-Bromobut-1-ene-1,2-diyl)dibenzene, a Key Intermediate of a Selective Estrogen Receptor Modulator. *Org. Process Res. Dev*. **2010**, *14* (5), 1147-1152.
( ) Tian, Q.; Cheng, Z.; Yajima, H. M.; Savage, S. J.; Green, K. L.; Humphries, T.; Reynolds, M. E.; Babu, S.; Gosselin, F.; Askin, D. A Practical Synthesis of a PI3K Inhibitor under Noncryogenic Conditions via Functionalization of a Lithium Triarylmagnesiate Intermediate. *Org. Process Res. Dev.* **2013**, *17* (1), 97-107.
( ) Beutner, G. L.; Hsiao, Y.; Razler, T.; Simmons, E. M.; Wertjes, W. Nickel-Catalyzed Synthesis of Quinazolinediones. *Org. Lett.* **2017**, *19* (5), 1052-1055.
(1) Wertjesa, W.; Ayersa, S.; Gaob, Q.; Simmons, E. M.; Beutner, G. L. A Divergent Nickel-Catalyzed Synthesis of Quinazolinediones and Benzoxazinone Imines. *Synthesis* **2018**, *50* (22), 4453-4461.
(2) Goldfogel, M. J.; Guo, X.; Meléndez Matos, J. L.; Gurak, Jr., J. A.; Joannou, M. V.; Moffat, W. B.; Simmons, E. M.; Wisniewski, S. R. Advancing Base-Metal Catalysis: Development of a Screening Method for Nickel-Catalyzed Suzuki–Miyaura Reactions of Pharmaceutically Relevant Heterocycles. *Org. Process Res. Dev*. **2022**, *26* (3), 785-794.
( ) Guo, X.; Dang, H.; Wisniewski, S. R.; Simmons, E. M. Nickel-Catalyzed Suzuki–Miyaura Cross-Coupling Facilitated by a Weak

Amine Base with Water as a Cosolvent. *Organometallics* **2022**, *41* (11), 1269-1274.
( ) West, M. J.; Watson, A. J. B. Ni vs. Pd in Suzuki–Miyaura sp^2–sp^2 cross-coupling: a head-to-head study in a comparable precatalyst/ligand system. *Org. Biomol. Chem.* **2019**, *17* (20), 5055-5059.
( ) Haibach, M. C.; Ickes, A. R.; Tcyrulnikov, S.; Shekhar, S.; Monfette, S.; Swiatowiec, R.; Kotecki, B. J.; Wang, J.; Wall, A. L.; Henry, R. F.; Hansen, E. C. Enabling Suzuki-Miyaura coupling of Lewis-basic arylboronic esters with a nonprecious metal catalyst. *Chem. Sci.* **2022**, *13* (43), 12906-12912.
( ) Burg, F.; Egger, J.; Deutsch, J.; Guimond, N. A Homogeneous Method for the Conveniently Scalable Palladium- and Nickel-Catalyzed Cyanation of Aryl Halides. *Org. Process Res. Dev.* **2016**, *20* (8), 1540-1545.
( ) Hethcox, J. C.; Kim, J.; Johnson, H. C.; Ji, Y.; Chow, M.; Newman, J. A.; DiRocco, D. A.; McMullen, J. P. Evolution of a Green and Sustainable Manufacturing Process for Belzutifan: Part 2—Development of a Scalable Nickel-Catalyzed Sulfonylation. *Org. Process Res. Dev.* **2024**, *28* (2), 413-421.
( ) Desrosiers, J. N.; Wei, X.; Gutierrez, O.; Savoie, J.; Qu, B.; Zeng, X.; Lee, H.; Grinberg, N.; Haddad, N.; Yee, N. K.; Roschangar, F.; Song, J. J.; Kozlowski, M. C.; Senanayake, C. H. Nickel-catalyzed C-3 direct arylation of pyridinium ions for the synthesis of 1-azafluorenes. *Chem. Sci.,* **2016**, *7*, 5581-5586.
( ) Fitzgerald, M. A.; Soltani, O.; Wei, C.; Skliar, D.; Zheng, B.; Li, J.; Albrecht, J.; Schmidt, M.; Mahoney, M.; Fox, R. J.; Tran, K.; Zhu, K.; Eastgate, M. D. Ni-Catalyzed C–H Functionalization in the Formation of a Complex Heterocycle: Synthesis of the Potent JAK2 Inhibitor BMS-911543. *J. Org. Chem.* **2015**, *80* (12), 6001-6011.
( ) Nimmagadda, S. K.; Korapati, S.; Dasgupta, D.; Malik, N. A.; Vinodini, A.; Gangu, A. S.; Kalidindi, S.; Maity, P.; Bondigela, S. S.; Venu, A.; Gallagher, W. P.; Aytar, S.; Bobes, F. G.; and Vaidyanathan, R. Development and Execution of an Ni(II)-Catalyzed Reductive Cross-Coupling of Substituted 2-Chloropyridine and Ethyl 3-Chloropropanoate. *Org. Process Res. Dev*. **2020**, *24* (6), 1141-1148.
(1) Yuan, N.; Jiang, Q.; Li, J.; Tang, J. A review on non-noble metal based electrocatalysis for the oxygen evolution reaction. *Arab. J. Chem.* **2020**, *13* (2), 4294-4309.
(2) Abdiaj, I.; Fontana, A.; Gomez, M. V.; de la Hoz, A.; Alcázar, J. Visible-Light-Induced Nickel-Catalyzed Negishi Cross-Couplings by Exogenous-Photosensitizer-Free Photocatalysis. *Angew. Chem. Int. Ed*. **2018**, *57* (28), 8473-8477.
( ) Liu, Y.; Wang. Y.; Qiu, Y. Electroreductive Cross-Electrophile Coupling (eXEC) Reactions. *Angew. Chem. Int. Ed.* **2023**, *62* (45), e202306679.
( ) Twilton, J.; Johnson, M. R.; Sidana,V.; Franke, M. C.; Bottecchia, C.; Lehnherr, D.; Lévesque, F.; Knapp, S. M. M.; Wang, L.; Gerken, J. B.; Hong, C. M.; Vickery, T. P.; Weisel, M. D.; Strotman, N. A.; Weix, D. J.; Root, T. W.; Stahl, S. S. Quinone-mediated hydrogen anode for non-aqueous reductive electrosynthesis. *Nature*, **2023**, *623*, 71-76.
( ) Shevlin, M.; Friedfeld, M. R.; Sheng, H.; Pierson, N. A.; Hoyt, J. M.; Campeau, L. C.; Chirik, P. J. Nickel-Catalyzed Asymmetric Alkene Hydrogenation of α,β-Unsaturated Esters: High-Throughput Experimentation-Enabled Reaction Discovery, Optimization, and Mechanistic Elucidation. *J. Am. Chem. Soc.* **2016**, *138* (10), 3562-3569.
( ) (a) Ullmann, F.; Bielecki, Ueber synthesen in der biphenylreihe. J. *Ber. Dtsch. Chem. Ges.* **1901**, *34*, 2174; (b) Goldberg, I. Ueber phenylirungen bei gegenwart von kupfer als katalysator. *Ber. Dtsch. Chem. Ges.* **1906**, 39 (2), 1691-1692.
( ) Bhunia, S.; Pawar, G. G.; Kumar, S. V.; Jiang, Y.; Ma, D. Selected Copper-Based Reactions for C–N, C–O, C–S, and C–C Bond Formation. *Angew. Chem. Int. Ed.* **2017**, *56* (51), 16136-16179.
( ) Joseph, P. J. A.; Priyadarshini, S. Copper-Mediated C–X Functionalization of Aryl Halides. *Org. Process Res. Dev.* **2017**, *21* (12), 1889-1924.
( ) Brown, A. T.; Riley, N. K. D. *Copper catalysis for pyridines and pyrimidines*, Elsevier, **2021**, pp. 115-159.
( ) Shivani, T.; Rakhi, M.; Rupa, M.; and Avijit, M.; Current Market Potential and Prospects of Copper-based Pyridine Derivatives: A Review, Current Molecular Medicine 2023; 23 () . https://dx.doi.org/10.2174/1566524023666230726160056
(1) Brewer, A. C.; Hoffman, P. C.; Martinelli, J. R.; Kobierski, M. E.; Mullane, N.; Robbins, D. Development and Scale-Up of a Continuous Aerobic Oxidative Chan–Lam Coupling. *Org. Process Res. Dev.* **2019**, *23* (8), 1484-1498.
(2) Steves, J. E.; Preger, Y.; Martinelli, J. R.; Welch, C. J.; Root, T. W.; Hawkins, J. M.; Stahl, S. S.; Process Development of CuI/ABNO/NMI-Catalyzed Aerobic Alcohol Oxidation. *Org. Process Res. Dev.* **2015**, *19* (11), 1548-1553.
( ) Ochen, A.; Whitten, R.; Aylott, H. E.; Ruffel, K.; Williams, G. D.; Slater, F.; Roberts, A.; Evans, P.; Steves, J. E.; Sanganee, M. J. Development of a Large-Scale Copper(I)/TEMPO-Catalyzed Aerobic Alcohol Oxidation for the Synthesis of LSD1 Inhibitor GSK2879552. *Organometallics* **2019**, *38* (1), 176-184.
( ) Osterberg, P. M.; Niemeier, J. K.; Welch, C. J.; Hawkins, J. M.; Martinelli, J. R.; Johnson, T. E.; Root, T. W.; Stahl, S. S. Experimental Limiting Oxygen Concentrations for Nine Organic Solvents at Temperatures and Pressures Relevant to Aerobic Oxidations in the Pharmaceutical Industry. *Org. Process. Res. Dev.* **2015**, *19* (11), 1537-1543.
( ) Gavriilidis, A.; Constantinou, A.; Hellgardt, K.; Hii, K. K. (Mimi); Hutchings, G. J.; Brett, G. L.; Kuhnd, S.; Marsden, S. P. Aerobic oxidations in flow: opportunities for the fine chemicals and pharmaceuticals industries. *React. Chem. Eng.* **2016**, *1*, 595-612.
( ) Hone, C. A., Kappe, C. O. The Use of Molecular Oxygen for Liquid Phase Aerobic Oxidations in Continuous Flow. *Top Curr Chem (Z)* 377, 2 (2019). https://doi.org/10.1007/s41061-018-0226-z.
( ) Witt, A.; Teodorovic, P.; Linderberg, M.; Johansson, P.; Minidis, A. A Novel Scalable Process to the GSK3β Inhibitor AZD8926 Based on a Heterocyclic Ziegler Coupling. *Org. Process Res. Dev*. **2013**, *17* (4), 672-678.
( ) Ruff, Y.; Berst, F. Efficient copper-catalyzed amination of DNA-conjugated aryl iodides under mild aqueous conditions. *Med. Chem. Commun*., **2018**, *9*, 1188-1193.
( ) Zhai, K.; Huang, Z.; Huang, Q.; Tao, W.; Fang, X.; Zhang, A.; Li, X.; Stark, G. R.; Hamilton, T. A.; Bao, S. Pharmacological inhibition of BACE1 suppresses glioblastoma growth by stimulating macrophage phagocytosis of tumor cells. *Nat Cancer* **2021**, *2*, 1136-1151.
( ) (a) Thaisrivongs, D. A.; Miller, S. P.; Molinaro, C.; Chen, Q.; Song, Z. J.; Tan, L.; Chen, L.; Chen, W.; Lekhal, A.; Pulicare, S. K.; Xu, Y. Synthesis of Verubecestat, a BACE1 Inhibitor for the Treatment of Alzheimer's Disease. *Org. Lett.* **2016**, *18* (22), 5780-5783; (b) Thaisrivongs, D. A.; Morris, W. J.; Tan, L.; Song, Z. J.; Lyons, T. W.; Waldman, J. H.; Naber, J. R.; Chen, W.; Chen, L.; Zhang, B.; Yang, J. A Next Generation Synthesis of BACE1 Inhibitor Verubecestat (MK-8931). *Org. Lett.* **2018**, *20* (6), 1568-1571; (c) Phillips, E. M.; Reibarkh, M.; Limanto, J.; Kieu, M.; Lekhal, A.; Zewge, D. Improved Process for a Copper-Catalyzed C–N Coupling in the Synthesis of Verubecestat. *Org. Process Res. Dev.* **2019**, *23* (8), 1674-1678.
(1) Baldwin, A. F.; Caporello, M. A.; Chen, G.; Goetz, A. E.; Hu, W.; Jin, C.; Knopf, K. M.; Li, Z.; Lu, C. V.; Monfette, S.; Puchlopek-Dermenci, A. L. A.; Shi, F. Kilogram-Scale Preparation of an Aminopyrazole Building Block via Copper-Catalyzed Aryl Amidation. *Org. Process Res. Dev.* **2021**, *25* (4), 1065-1073.
(2) Peng, F.; McLaughlin, M.; Liu, Y.; Mangion, I.; Tschaen, D. M.; Xu, Y. A Mild Cu(I)-Catalyzed Oxidative Aromatization of Indolines to Indoles. *J. Org. Chem.* **2016**, *81* (20), 10009-10015.
( ) Gallagher, W. P.; Soumeillant, M.; Chen, K.; Fox, R. J.; Hsiao, Y.; Mack, B.; Iyer, V.; Fan, J.; Zhu, J.; Beutner, G.; Silverman, S. M.; Fanfair, D. D.; Glace, A. W.; Freitag, A.; Sweeney, J.; Ji, Y.; Blackmond, D. G.; Eastgate, M. D.; Conlon, D. A. Preparation of the HIV Attachment Inhibitor BMS-663068. Part 7. Development of a Regioselective Ullmann–Goldberg–Buchwald Reaction. *Org. Process Res. Dev.* **2017**, *21* (8), 1156-1165.
( ) Fantasia, S.; Bartels, B.; Bliss, F.; Koch, F.; Scalone, M.; Spiess, D.; Steiner, M.; Wang, S.; Püntener, K. A Streamlined, Safe and

Sustainable Process for Gemlapodect. *Helv. Chim. Acta,* **2023**, 106 (10), e202300116.
( ) Peng, F.; Chen, Y.; Chen, C.; Dormer, P. G.; Kassim, A.; McLaughlin, M.; Reamer, R. A.; Sherer, E. C.; Song, Z. J.; Tan, L.; Tudge, M. T.; Wan, B.; Chung, J. Y. L. Asymmetric Formal Synthesis of the Long-Acting DPP-4 Inhibitor Omarigliptin. *J. Org. Chem.* **2017**, *82* (17), 9023-9029.
( ) Peng, F; Humphrey, G. R.; Maloney, K. M.; Lehnherr, D.; Weisel, M.; Lévesque, F.; Naber, J. R.; Brunskill, A. P. J.; Larpent, P.; Zhang, S.-W.; Lee, A. Y.; Arvary, R. A.; Lee, C. H.; Bishara, D.; Narsimhan, K.; Sirota, E.; Whittington, M. Development of a Green and Sustainable Manufacturing Process for Gefapixant Citrate (MK-7264) Part 2: Development of a Robust Process for Phenol Synthesis. *Org. Process Res. Dev.* **2020**, *24* (11), 2453-2461.
( ) Fier, P. S.; Maloney, K. M. Reagent Design and Ligand Evolution for the Development of a Mild Copper-Catalyzed Hydroxylation Reaction. *Org. Lett.* **2017**, *19* (11), 3033-3036.
( ) Hartung, J. S.; Greszler, N.; Klix, R. C.; Kallemeyn, J. M. Development of an Enantioselective [3+2] Cycloaddition To Synthesize the Pyrrolidine Core of ABBV-3221 on Multikilogram Scale. *Org. Process Res. Dev*. **2019**, *23* (11), 2532-2537.
( ) (a) Moon, S. J.; Govindan, S. V.; Cardillo, T. M.; D'Souza, C. A.; Hansen, H. J.; Goldenberg, D. M. *J. Med. Chem*. **2008**, 51 (21), 6916-6926. (b) Govindan, S. V.; Goldenberg, D. M. Camptothecin conjugates of anti-CD22 antibodies for treatment of B cell diseases. US 2013/8420086 B2, **2013**. (c) Govindan, S. V.; Goldenberg, D. M. Dosages of immunoconjugates of antibodies and SN-38 for improved efficacy and decreased toxicity US 2015/9028833 B2, **2015**.
(100) Li, X.; Yang, Q.; Lorsbach, B. A.; Buysse, A.; Niyaz, N.; Cui, L.; Ross, R., Jr., Toward the Development of a Manufacturing Process for the Insecticide Tyclopyrazoflor. Part I. Evaluation of Strategies using Ullmann Coupling of Pyrazole Derivatives. *Org. Process Res. Dev*. **2022**, *26* (12), 3290-3302.
(101) Yu, H.; Yang, H.; Chen, L.; Wang, G.; Zhao, G.; Wang, X.; Wu, H.; Shi, X.; Dong, Y.; Li, B. Route Design and Development of Tetrachlorantraniliprole: Copper-Catalyzed Cyclization and One-Pot Preparation of Pyrazole Acid Chloride. *Org. Process Res. Dev.* **2022**, *26* (12), 3216-3225.
(102) (a) Liu, J.; Han, Z.; Wang, X.; Wang, Z.; Ding, K. Highly Regio- and Enantioselective Alkoxycarbonylative Amination of Terminal Allenes Catalyzed by a Spiroketal-Based Diphosphine/Pd(II) Complex. *J. Am. Chem. Soc.* **2015**, *137* (49), 15346-15349. (b) Pletsas, D.; Garelnabi, E. A. E.; Li, L.; Phillips, R. M.; Wheelhouse, R. T. Synthesis and Quantitative Structure–Activity Relationship of Imidazotetrazine Prodrugs with Activity Independent of O6-Methylguanine-DNA-methyltransferase, DNA Mismatch Repair, and p53. *J. Med. Chem.* **2013**, *56* (17), 7120-7132.
(1) Fandrick, D. R.; Fandrick, K. R.; Reeves, J. T.; Tan, Z.; Tang, W.;
Capacci, A. G.; Rodriguez, S.; Song, J. J.; Lee, H.; Yee, N. K.; Senanayake, C. H. Copper Catalyzed Asymmetric Propargylation of Aldehydes. *J. Am. Chem. Soc.* **2010**, *132* (22), 7600-7601.
(1) Gaspar, B.; Carreira, E. M. Mild Cobalt-Catalyzed Hydrocyanation of Olefins with Tosyl Cyanide. *Angew. Chem. Int. Ed.* **2007**, *46* (24), 4519-4522.
(1) Girijavallabhan, V.; Alvarez, C.; Njoroge, F. G. Regioselective Cobalt-Catalyzed Addition of Sulfides to Unactivated Alkenes. *J. Org. Chem.* **2011**, *76* (15), 6442-6446.
(1) Hayashi, T.; Kikuchi, S.; Asano, Y.; Endo, Y.; Yamada, T. Homogeneous Enantioselective Catalysis in a Continuous-Flow Microreactor: Highly Enantioselective Borohydride Reduction of Ketones Catalyzed by Optically Active Cobalt Complexes. *Org. Process Res. Dev.* **2012**, *16* (6), 1235-1240.
(1) Pangu, A. J.; Cohen, R. D.; Tudge, M. T.; Chen, Y. Dearomatization of Electron-Deficient Nitrogen Heterocycles via Cobalt-Catalyzed Asymmetric Cyclopropanation. *J. Org. Chem.* **2016**, *81* (8), 3070-3075.
(1) Berger, K. E.; Martinez, R. J.; Zhou, J.; Uyeda, C. Catalytic Asymmetric Cyclopropanations with Nonstabilized Carbenes. *J. Am. Chem. Soc.* **2023**, *145* (17), 9441-9447.
(1) Algera, R. F.; Allais, C.; Baldwin, A. F.; Busch, T.; Colombo, F.; Colombo, M.; Depretz, C.; Dumond, Y. R.; Faria Quintero, A. R.; Heredia, M.; Jung, J.; Lall, A.; Lee, T.; Liu, Y.; Mandelli, S.; Mantel, M.; Morris, R.; Mustakis, J.; Nguyen, B.; Pearson, R.; Piper, J. L.; Ragan, J. A.; Ruffin, B.; Talicska, C.; Tcyrulnikov, S.; Uyeda, C.; Weekly, R. M.; Zeng, M. Synthesis of Nirmatrelvir: Development of a Scalable Cobalt-Catalyzed Cyclopropanation for Manufacture of the Bicyclic [3.1.0]Proline-Building Block. *Org. Process. Res. Dev.* **2023**, *27* (12), 2260-2270.
(11) Friedfeld, M. R.; Zhong, H.; Ruck, R. T.; Shevlin, M.; Chirik, P. J. Cobalt-catalyzed asymmetric hydrogenation of enamides enabled by single-electron reduction. *Science* **2018**, *360* (6391), 888-893.
(111) Surtees, J.; Marmon, V.; Differding, E.; Zimmerman, V. 2-OXO-1-PYRROLIDINE DERIVATIVES, PROCESS FOR PREPARING THEM AND THEIR USES. PCT international application patent WO 2001064637 A1 (2001).
(112) Du, X.; Xiao, Y.; Huang, J. M.; Zhang, Y.; Duan, Y. N.; Wang, H.; Shi, C.; Chen, G. Q.; Zhang, X. Cobalt-catalyzed highly enantioselective hydrogenation of α,β-unsaturated carboxylic acids. *Nat. Commun.,* **2020**, *11*, 3239.
(11) Zhong, H.; Shevlin, M.; Chirik, P. J. Cobalt-Catalyzed Asymmetric Hydrogenation of α,β-Unsaturated Carboxylic Acids by Homolytic H2 Cleavage. *J. Am. Chem. Soc*. **2020**, *142* (11), 5272-5281.
(11) (a) Gazal, S.; Gupta, P.; Gunturu, S. R.; Isherwood, M.; Voss, M. E. Application of Isayama–Mukaiyama cobalt catalyzed hydroperoxysilylation for the preparation of ritonavir hydroperoxide. *Tetrahedron Lett*. **2016**, *57* (46), 5099-5102; (b) O'Neill, P. M.; Hindley,; Pugh, S. M. D.; Davies, J.; Bray, P. G.; Park, B. K.; Kapu, D. S.; Ward, S. A.; Stocks, P. A. Co(thd)2: a superior catalyst for aerobic epoxidation and hydroperoxysilylation of unactivated alkenes: application to the synthesis of spiro-1,2,4-trioxanes. *Tetrahedron Letters*, **2003**, *44* (44), 8135-8138.
(11) Xiao, S.; Ai, L.; Liu, Q.; Yang, B.; Huang, J.; Xue, W.; Chen, Y. Total Synthesis of Natural Terpenoids Enabled by Cobalt Catalysis. *Front. Chem.,* **2022**, *10*, 941184.
(11) Hoyt, J. M.; Shevlin, M.; Margulieux, G. W.; Krska, S. W.; Tudge, M. T.; Chirik, P. J. Synthesis and Hydrogenation Activity of Iron Dialkyl Complexes with Chiral Bidentate Phosphines. *Organometallics* **2014**, *33*, 5781-5790.
(11) Shang, R.; Ilies, L.; Nakamura, E. Iron-Catalyzed C–H Bond Activation. *Chem. Rev*. **2017**, *117* (13), 9086-9139.
(11) Cera, G.; Ackermann, L. Iron-Catalyzed C-H Functionalization Processes. *Top Curr Chem* (Z) 374, 57 (2016). https://doi.org/10.1007/s41061-016-0059-6.
(11) Risatti, C.; Natalie, K. J.; Shi, Z. Conlon, D. A. Development of a Scalable Route to a Dual NK-1/Serotonin Receptor Antagonist. *Org. Process Res. Dev.* **2013**, *17* (2), 257-264.
(12) Tewari, N.; Maheshwari, N.; Medhane, R.; Nizar, H.; Prasad, M. A Novel Method for the Large Scale Synthesis of Cinacalcet Hydrochloride Using Iron Catalyzed C–C Coupling. *Org. Process Res. Dev*. **2012**, *16* (9), 1566-1568.
(121) Ruda, A. M.; Papadouli, S.; Thangavadivale, V.; Moseley, J. D. Application of the Polonovski Reaction: Scale-up of an Efficient and Environmentally Benign Opioid Demethylation. *Org. Process Res. Dev*. **2022**, *26* (5), 1398-1404.
(122) Buono, F. G.; Zhang, Y.; Tan, Z.; Brusoe, A.; Yang, B. S.; Lorenz, J. C.; Giovannini, R.; Song, J. J.; Yee, N. K.; Senanayake, C. H. Efficient Iron-Catalyzed Kumada Cross-Coupling Reactions Utilizing Flow Technology under Low Catalyst Loadings. *Eur. J. Org. Chem.* **2016**, 2016 (15), 2599-2602.
(12) Shevlin, M.; Guan, X.; Driver, T. G. Iron-Catalyzed Reductive Cyclization of o-Nitrostyrenes Using Phenylsilane as the Terminal Reductant. *ACS Catal.* **2017**, *7* (8), 5518-5522.
(12) Tondreau, A. M.; Atienza, C. C. H.; Weller, K. J.; Nye, S. A.; Lewis, K. M.; Delis, J. G. P.; Chirik, P. J. Iron Catalysts for Selective Anti-Markovnikov Alkene Hydrosilylation Using Tertiary Silanes. *Science* **2012**, *335* (6068), 567-570.

(12) Turner, O. J.; Murphy, J. A.; Hirst, D. J.; Talbot, E. P. A. Hydrogen Atom Transfer-Mediated Cyclisations of Nitriles. *Chem. Eur. J.* **2018**, *24* (70), 18658-18662.
(12) Chen, C.; He, F.; Tang, G.; Yuan, H.; Li, N.; Wang, J.; Faessler, R. Synthesis of Quinazolines via an Iron-Catalyzed Oxidative Amination of N-H Ketimines. *J. Org. Chem*. **2018**, *83* (4), 2395-2401.
(12) Zhou, B.; Chen, H.; Wang, C. Mn-Catalyzed Aromatic C-H Alkenylation with Terminal Alkynes. *J. Am. Chem. Soc.* **2013**, *135* (4), 1264-1267.
(12) Wang, Y.; Wang, M.; Li, Y.; Liu, Q. Homogeneous manganese-catalyzed hydrogenation and dehydrogenation reactions. *Chem* **2021**, *7*, 1180-1223.
(12) He, R.; Jin, X.; Chen, H.; Huang, Z. T.; Zheng, Q, Y.; Wang, C. Mn-Catalyzed Three-Component Reactions of Imines/Nitriles, Grignard Reagents, and Tetrahydrofuran: An Expedient Access to 1,5-Amino/Keto Alcohols. *J. Am. Chem. Soc.* **2014**, *136* (18), 6558-6561.
(1) Wang, J.; Zheng, K.; Li, T.; Zhan, X. Mechanism and Chemoselectivity of Mn-Catalyzed Intramolecular Nitrene Transfer Reaction: C–H Amination vs. C=C Aziridination. *Catalysts* **2020**, *10 (3)*, 292.
(1 1) Inoki, S.; Kato, K.; Mukaiyama, T. A new and facile for the direct preparation of α-hydroxycarboxylic acid esters from α,β-unsaturated carboxylic acid esters with molecular oxygen and phenylsilane catalyzed by bis(dipivaloylmethanato)manganese(II) complex. *Chem. Lett*. **1990**, *19* (10)1869-1872.
(1 2) (a) Magnus, P.; Waring, M. J.; Scott, D. A. Conjugate reduction of α,β-unsaturated ketones using an Mn^{III} catalyst, phenylsilane and isopropyl alcohol. *Tetrahedron Lett*. **2000**, *41* (50), 9731-9733; (b) Magnus, P.; Payne, A. H.; Hobson, L. Synthesis of the Kopsia alkaloids (±)-11,12-demethoxylahadinine B, (±)-kopsidasine and (±)-kopsidasine-N-oxide. *Tetrahedron Lett.* **2000**, *41* (13), 2077-2081.
(1) Snider, B. B. Manganese(III)-Based Oxidative Free-Radical Cyclizations. *Chem. Rev*. **1996**, *96* (1), 339-364.
(1) Cassayre, J.; Winkler, T.; Pitterna, T.; Quaranta, L. Application of Mn(III)-catalysed olefin hydration reaction to the selective functionalisation of avermectin B1. *Tetrahedron Lett*. **2010**, *51* (13), 1706-1709.
(1) Sortais, J. B.; Buhaibeh, R.; Canac, Y. Manganese-Catalyzed Hydrogenation and Hydrogen Transfer Reactions. In *Manganese Catalysis in Organic Synthesis*, J. B. Sortais (Ed.), **2021**, Wiley-VCH, Weinheim.
(1) (a) Green, S. A.; Crossley, S. W. M.; Matos, J. L. M.; Vásquez-Céspedes, S.; Shevick, S. L.; Shenvi, R. A. The High Chemofidelity of Metal-Catalyzed Hydrogen Atom Transfer. *Acc. Chem. Res.* **2018**, *51* (11), 2628-2640. (b) King, S. M.; Ma, X.; Herzon, S. B. A Method for the Selective Hydrogenation of Alkenyl Halides to Alkyl Halides. *J. Am. Chem. Soc*. **2014**, *136* (19), 6884-6887.
(1) Smejkal, T.; Gopalsamuthiram, V.; Ghorai, S. K.; Jawalekar, A. M.; Pagar, D.; Sawant, K.; Subramanian, S.; Dallimore, J.; Willetts, N.; Scutt, J. N.; Whalley, L.; Hotson, M.; Hogan, A. M.; Hodges, G. Optimization of Manganese Coupling Reaction for Kilogram-Scale Preparation of Two Aryl-1,3-dione Building Blocks. *Org. Process Res. Dev.* **2017**, *21* (10), 1625-1632.
(1) Nuhant, P.; Oderinde, M. S.; Genovino, J.; Juneau, A.; Gagné, Y.; Allais, C.; Chinigo, G. M.; Choi, C.; Sach, N. W.; Bernier, L.; Fobian, Y. M.; Bundesmann, M. W.; Khunte, B.; Frenette, M.; Fadeyi, O. O. Visible-Light-Initiated Manganese Catalysis for C-H Alkylation of Heteroarenes: Applications and Mechanistic Studies. *Angew. Chem. Int. Ed.* **2017**, *56* (48), 15309-15313.
(1) Food and Drug Administration Carfilzomib. July 20, 2012. Available at: www.fda.gov/Drugs/InformationOnDrugs/ApprovedDrugs/ucm312945.htm.
(1) (a) Dornan, P. K.; Anthoine, T.; Beaver, M. G.; Cheng, G. C.; Cohen, D. E.; Cui, S.; Lake, W. E.; Langille, N. F.; Lucas, S. P.; Patel, J.; Powazinik IV, W.; Roberts, S. W.; Scardino, C.; Tucker, J. L.; Spada, S.; Zeng, A.; Walk, S. D. Continuous Process Improvement in the Manufacture of Carfilzomib, Part 1: Process Understanding and Improvements in the Commercial Route to Prepare the Epoxyketone Warhead. *Org. Process Res. Dev.* **2020**, *24* (4), 481-489; (b) Beaver, M. G.; Shi, X.; Riedel, J.; Patel, P.; Zeng, A.; Corbett, M. T.; Robinson, J. A.; Parsons, A. T.; Cui, S.; Baucom, K.; Lovette, M. A.; Içten, E.; Brown, D. B.; Allian, A.; Flick, T. G.; Chen, W.; Yang, N.; Walker, S. D. Continuous Process Improvement in the Manufacture of Carfilzomib, Part 2: An Improved Process for Synthesis of the Epoxyketone Warhead. *Org. Process Res. Dev.* **2020**, *24* (4), 490-499; (c) Maloney, A. J.; Içten, E.; Capellades, G.; Beaver, M. G.; Zhu, X.; Graham, L. R.; Brown, D. B.; Griffin, D. J.; Sangodkar, R.; Allian, A.; Huggins, S.; Hart, R.; Rolandi, P.; Walker, S. D.; Braatz, R. D. A Virtual Plant for Integrated Continuous Manufacturing of a Carfilzomib Drug Substance Intermediate, Part 3: Manganese-Catalyzed Asymmetric Epoxidation, Crystallization, and Filtration. *Org. Process Res. Dev.* **2020**, *24* (10), 1891-1908.
(1 1) (a) Wei, Z.; Li, H.; Wang, Y.; Liu, Q. A Tailored Versatile and Efficient NHC-Based NNC-Pincer Manganese Catalyst for Hydrogenation of Polar Unsaturated Compounds. *Angew. Chem. Int. Ed.* **2023**, *62*, e202301042; (b) Liu, C.; Wang, M.; Xu, Y.; Li, Y.; Liu, Q. Manganese-Catalyzed Asymmetric Hydrogenation of 3H-Indoles. *Angew. Chem. Int. Ed.* **2022**, *61*, e202202814.
(1 2) Enthaler, S. Rise of the Zinc Age in Homogeneous Catalysis? *ACS Catal*. **2013**, *3 (2)*, 150-158.
(1) Monfette, S.; Fang, Y.-Q.; Bio, M. M.; Brown, A. R.; Crouch, I. T.; Desrosiers, J.-N.; Duan, S.; Hawkins, J. M.; Hayward, C. M.; Peperni, N.; Rainville, J. P. Continuous Process for Preparing the Difluoromethylating Reagent [(DMPU)2Zn(CF2H)2] and Improved Synthesis of the ICHF2 Precursor. *Org. Process Res. Dev*. **2020**, *24* (6), 1077-1083.
(1) Serizawa, H.; Ishii, K.; Aikawa, K.; Mikami, K. Copper-Catalyzed Difluoromethylation of Aryl Iodides with (Difluoromethyl)zinc Reagent. *Org. Lett.* **2016**, *18* (15), 3686-3689.
(1) Aikawa, K.; Ishii, K.; Endo, Y.; Mikami, K. Copper-catalyzed allylic difluoromethylation of allyl carbonates with (difluoromethyl)zinc reagent. *J. Fluorine Chem.* **2017**, *203*, 122-129.
(1) Xu, L.; Vicic, D. A. Direct Difluoromethylation of Aryl Halides via Base Metal Catalysis at Room Temperature. *J. Am. Chem. Soc*. **2016**, *138* (8), 2536-2539.
(1) Bundesmann, M. W.; Coffey, S. B.; Wright, S. W., Amidation of esters assisted by $Mg(OCH_3)_2$ or $CaCl_2$. *Tetrahedron Letters* **2010**, *51* (30), 3879-3882.
(148) (a) Rochat, R.; Lopez, M. J.; Tsurugi, H.; Mashima, K. Recent Developments in Homogeneous Organomagnesium Catalysis. *ChemCatChem* **2016**, *8* (1), 10-20; (b) Yang, D.; Wang, L.; Li D.; Wang, R. Magnesium Catalysis in Asymmetric Synthesis. *Chem* **2019**, *5*, 1108-1166.
(1) (a) Czombik, M.; Gajewy, J.; Czapik, A.; Kwit, M. Magnesium-catalyzed stereoselective transformations – A survey through recent achievements. *Polyhedron* **2022**, *219*, 115790.
(1) Weetman, C.; Hill, M. S.; Mahon, M. F. Magnesium Catalysis for the Hydroboration of Carbodiimides. *Chem. Eur. J.* **2016**, *22* (21), 7158-7162.
(1 1) Sim, J. T.; Kim, S. G. Asymmetric Synthesis of 1,1-Diarylalkanes via Friedel–Crafts Alkylation of Donor–Acceptor Cyclopropanes with Electron-Rich Benzene. *J. Korean Chem. Soc.,* **2016**, *60* (5), 374-377.
(1 2) Li, D.; Wang, K.; Wang, L.; Wang, Y.; Wang, P.; Liu, X.; Yang, D.; Wang, R. Enantioselective Oxidative Ring-Opening Reaction of Aziridines with α-Nitroesters Using Cinchona Alkaloid Amide/Nickel(II) Catalysts. *Org. Lett.* **2017**, *19* (1), 3211-3214.
(1) (a) Magre, M.; Szewczyk, M.; Rueping, M. N-Methylation and Trideuteromethylation of Amines via Magnesium-Catalyzed Reduction of Cyclic and Linear Carbamates. *Org. Lett.* **2020**, *22* (8), 3209-3214. (b) Jang, Y. K.; Magre, M.; Rueping, M. Chemoselective Luche-Type Reduction of α,β-Unsaturated Ketones by Magnesium Catalysis. *Org. Lett.* **2019**, *21* (20), 8349-8352.
(1) (a) Möhle, S.; Zirbes, M.; Rodrigo, E.; Gieshoff, T.; Wiebe, A.; Waldvogel, S. R. Modern Electrochemical Aspects for the Synthesis of Value-Added Organic Products. *Angew. Chem. Int. Ed.* **2018**, *57* (21), 6018-6041. (b) Lehnherr, D.; Chen, L. Overview of Recent Scale-Ups in Organic Electrosynthesis (2000–2023). *Org. Process. Res. Dev.* **2024**, *28* (2), 338-366.

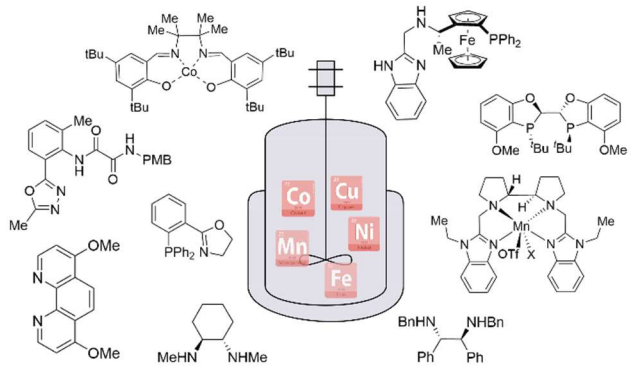
Co
Cu
Mn
Ni
Fe
PMB
OMe
MeHN
NHMe
BnHN
NHBn
Ph
Ph
OTf
X
Me
tBu
OMe